AD NUMBER

AD869093

NEW LIMITATION CHANGE

TO

Approved for public release, distribution unlimited

FROM

Distribution authorized to U.S. Gov't. agencies and their contractors; Critical Technology; FEB 1970. Other requests shall be referred to Army Aberdeen Research and Development Center, Aberdeen Proving Ground, MD 21005.

AUTHORITY

brl per dtic form 55

THEORETICAL CALCULATION OF ISO-DAMAGE CHARACTERISTICS

AD 869093

Joshua E. Greenspon, Dr. Eng.



Ballistic Research Laboratories
Aberdeen Proving Ground
Contract No. DAAD05-69-C-0116
Tech. Rep. No. 10
February, 1970



J G ENGINEERING RESEARCH ASSOCIATES
3831 MENLO DRIVE BALTIMORE, MARYLAND 21215



49

# DISCLAIMER NOTICE

ABSTRACT

This report contains methods for constructing iso-damage curves for structures. The results for the cylindrical shell are given in detail. It is shown that by starting with the theory presented here, we can derive the empirical relation developed by Johnson several years ago. The theory of damage due to short duration contact explosion is presented and the results are compared with experiment. A series of curves are presented which give the damage sensitivity of cylinders as a function of the ratios of diameter to thickness and length to diameter.

TABLE OF CONTENTS

ACKNOWLEDGEMENTS

This work was sponsored by the Ballistic Research Laboratories at Aberdeen Proving Ground. The technical supervisors of the project were Mr. O. T. Johnson and Dr. W. J. Schuman, Jr. The author is grateful to these gentlemen for their guidance and encouragement during the process of this work.

## LIST OF SYMBOLS

| | |
|---|---|
| $P, P_s$ | side on pressure |
| $I$ | side on impulse |
| $I_o$ | impulse below which no damage will occur |
| $P_o$ | pressure below which no damage will occur |
| $\bar{a}$ | time constant of exponentially decaying pressure |
| $p(t)$ | pressure as a function of time |
| $E_f$ | energy flux in explosion (i.e. energy per unit area in shock front) |
| $\rho_o$ | air density |
| $c_o$ | sound velocity in air |
| $V$ | total energy absorbed in structure |
| $E$ | total energy of explosion which is directed toward target |
| $A$ | projected area of target directed toward explosion |
| $\bar{A}$ | $2\rho_o c_o$ |
| $W$ | weight of explosive |
| $R$ | distance from explosion to target |
| $\bar{k}, \bar{\ell}, \bar{\alpha}, \bar{\beta}$ | constants which describe the pressure and impulse as a function of W and R |
| $T$ | positive duration of overpressure |
| $f_1(P_s), f_2(P_s)$ | nondimensional functions which describe the impulse and energy in a blast |
| $\bar{T}'$ | kinetic energy in the structure |
| $u, v, w$ | displacements of a point on the structure in three orthogonal directions |
| $V'$ | work done by internal forces in deforming the structure |
| $W'$ | work done by external forces |
| $X, Y, Z$ | components of the external force |
| $\bar{M}$ | generalized mass |
| $\bar{R}$ | generalized resistance function |
| $\bar{P}(t)$ | generalized force |
| $\mu$ | mass per unit area of structure |

| | |
|---|---|
| $f_w(A)$ | deflection distribution in the lateral plastic deformation pattern |
| $\bar{H}$ | impulse on the structure from the short duration explosion |
| $\sigma_x, \sigma_y, \sigma_z, \tau_{xy}, \tau_{xz}, \tau_{yz}$ | stresses in the structure |
| $\epsilon_x, \epsilon_y, \epsilon_z, \gamma_{xy}, \gamma_{xz}, \gamma_{yz}$ | strains in the structure |
| $\tau_o$ | oct hedral shear stress (3 dimensional) |
| $\gamma_o$ | oct hedral shear strain (3 dimensional) |
| $\sigma_i$ | oct hedral shear stress (biaxial) |
| $\epsilon_i$ | oct hedral shear strain (biaxial) |
| $\sigma_s$ | yield stress |
| $\bar{K}$ | slope of elastic-linear plastic material |
| $E$ | elastic modulus |
| $e_s$ | yield strain |
| $\bar{T}$ | absolute temperature |
| $\bar{T}_m$ | absolute melting temperature of metal |
| $Q', R', T'$ | powers of $e_i$ in the expression for the absorbed energy |
| $\sigma_x, \sigma_\varphi, \tau_{x\varphi}$ | biaxial stresses in a cylindrical shell |
| $\lambda$ | parameter describing strain hardening |
| $\nu$ | Poisson's ratio |
| $x, \varphi$ | cylindrical coordinates |
| $x'$ | $x/\ell$ |
| $h$ | shell thickness |
| $a$ | shell radius |
| $\ell, L$ | shell length |
| $N_x, N_\varphi, N_{x\varphi}$ | membrane forces in the cylinder (force per unit length) |
| $\alpha'$ | decay parameter for exponentially distributed loading on shell |
| $p_c$ | pressure at which collapse commences |
| $p_B$ | uniform pressure at which bucklong commences |
| $f_e, \bar{\varphi}, \beta_e, \beta_e', \theta_e$ | parameters used for the calculation of the buckling load |
| $p_B'$ | peak nonuniform pressure at which buckling commences |
| $\rho'$ | parameter describing distribution of pressure in a cylinder in buckling |

| | |
|---|---|
| $\bar{K}$ | correction factor to get nonuniform buckling pressure from uniform buckling pressure |
| $I_1$ | component of nondimensional energy in perfectly plastic material |
| $k$ | exponential decay constant for buckle shape |
| $n$ | number of full circumferential waves in buckling pattern |
| $w_m, w_0$ | maximum deflection of cylinder |
| $G, H, C, B, K$ | constants for the deflection pattern of a cylinder under contact explosion |
| $D$ | diameter of cylinder |
| $\rho$ | mass density of cylinder material |
| $\bar{I}$ | peak impulse per unit area in a $180^\circ$ cosine distribution of impulse |

## I. Introduction and background

The iso-damage concept was originated at Ballistic Research Laboratories in the early 1950's. Just as isothermal means constant temperature, so iso-damage means constant damage. The iso-damage curve consists of a plot of incident pressure as ordinate with incident impulse as abscissa such as shown in Fig. 1.

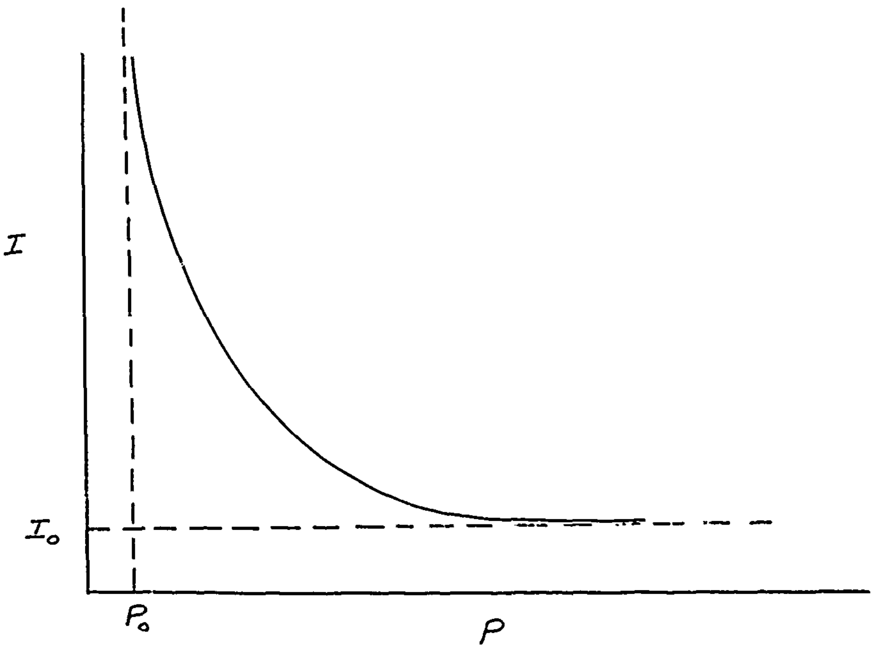


Fig. 1 Typical Iso-Damage Curve

The experimental iso-damage curve is formed by testing a structure under a series of explosive weights and distances of explosion to the target. For each explosive weight and distance a certain damage level will occur. A curve which is faired through the same damage level for various impulse and pressure is called an iso-damage curve. Each structure will have a series of these curves, one for each damage level. The asymptotes shown by the dotted lines are minimum values of pressure and impulse for which damage level A will occur. Thus for $I < I_0$, no matter what the value of P there will be no damage at "Damage Level A." Likewise for $P < P_0$ no matter what the level of I there will be no damage at "Damage Level A." There will be a series of asymptotes -- a pair for each damage level.

## II. Iso-damage theory

### A. General concepts

In a previous report[1*] iso-damage theory was illustrated by using the exponential decay curve as a first approximation. For example, assume that the pressure time relation is as follows:

*Superscripts refer to references listed at the end of the report.

$$p(t) = P e^{-t/\bar{a}}$$ [1]

where P denotes the maximum pressure and $\bar{a}$ is the time constant of the decay. The energy flux in the explosion at any point (i.e. the energy per unit area) is given by the expression[2]

$$E_f = \frac{1}{\rho_0 c_0} \int_0^{\infty} p(t)^2 dt = \frac{P^2 \bar{a}}{2 \rho_0 c_0}$$ [2]

where $\rho_0$ is the density of the medium and $c_0$ is the sound velocity in the medium. The impulse per unit area is given by [2]

$$I = \int_0^{\infty} p(t) dt = P\bar{a}$$ [3]

Thus

$$E_f = \frac{PI}{2\rho_0 c_0}$$ [4]

Neglecting any dissipation effects, the conservation of energy demands that the energy absorbed by the structure in deforming be equal to the energy directed to the structure from the explosion. The damage that occurs in the structure can be measured by the energy absorbed by the structure in deforming. Thus

$$V = E$$ [5]

where $V$ is the total energy absorbed by the structure and $E$ is the energy directed to the structure from the explosion. The total energy $E$ can be written in terms of the energy flux, $E_f$ by the expression

$$E = E_f A$$ [6]

where $A$ is the projected area of the structure directed toward the explosion.

The energy absorbed by the structure is equal to the internal work done by the structure in deforming. For a given level of damage (i.e. a given deflection distribution) there is a single value of internal work done by the structure. This means that the structure does a given amount of internal work which then results in a given plastic deflection distribution. Thus the damage in the structure is measured by the value of $V$. It is true that we can obtain the same value of for different deflection distributions. However for certain types of loads and structural geometries the patterns of plastic deflection are fixed. The maximum deflection in this fixed pattern of deformation is a measure of the magnitude of $V$ and therefore of damage to the structure. Thus

$$E_f = V/A$$ [7]

Substituting into [4]

$$PI = 2\rho_0 c_0 \frac{V}{A}$$ [8]

For the exponentially decaying pressure the iso-damage curves are hyperbolas as shown in Fig. 2:

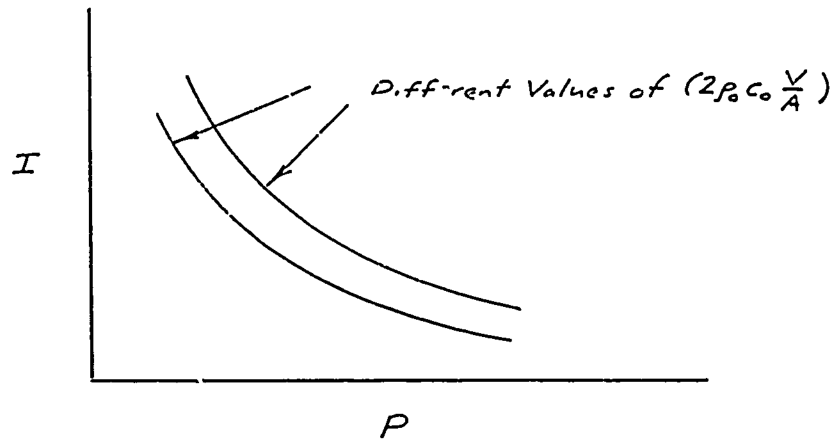


Fig. 2 Iso-Damage Curve with the Energy as a Parameter

B. Conceptual comparison with the Johnson Theory[3]

Recently O. T. Johnson of BRL offered a new theory of blast damage. Although Johnson derived his theory from empirical considerations, it can be shown that his theory is fundamentally well grounded. To prove this we start with the form of the iso-damage curve derived in the last section, i.e.

$$PI = \bar{A}\, E_f \qquad [9]$$

where $\bar{A}$ is a constant

Consider two tests, one with side on pressure $P_1$, impulse $I_1$, weight $W_1$ and distance from explosion to target $R_1$; the other with pressure $P_2$, impulse $I_2$, weight $W_2$ and distance $R_2$. In order for the same damage to occur in both tests the same energy has to be absorbed in the structure. Thus, for the same damage

$$P_1 I_1 = P_2 I_2 \qquad [10]$$

According to Cole[4] the pressure and impulse can be represented as a function of the explosive weight and distance by the general relations

$$P = \bar{k}\left(\frac{W^{1/3}}{R}\right)^{\bar{\alpha}} \qquad [11]$$

$$I = \bar{l}\, W^{1/3}\left(\frac{W^{1/3}}{R}\right)^{\bar{\beta}} \qquad [12]$$

where $\bar{k}, \bar{l}, \bar{\alpha}, \bar{\beta}$ are empirical constants.

Substituting [11] and [12] into [10] we obtain

$$\bar{k}\left(\frac{W_1^{1/3}}{R_1}\right)^{\bar{\alpha}} \bar{l}\, W_1^{1/3}\left(\frac{W_1^{1/3}}{R_1}\right)^{\bar{\beta}} = \bar{k}\left(\frac{W_2^{1/3}}{R_2}\right)^{\bar{\alpha}} \bar{l}\, W_2^{1/3}\left(\frac{W_2^{1/3}}{R_2}\right)^{\bar{\beta}} \qquad [13]$$

Thus

$$\frac{R_1}{R_2} = \left(\frac{W_1}{W_2}\right)^{\frac{\bar{\alpha}+\bar{\beta}+1}{3(\bar{\alpha}+\bar{\beta})}} \qquad [14]$$

From Goodman's curves[5] we obtain approximate values for $\bar{\alpha}$ and $\bar{\beta}$ i.e.

$$\bar{\alpha} \approx 1 \quad , \quad \bar{\beta} \approx 1$$

Thus

$$(R_1/R_2) \approx (W_1/W_2)^{.5} \qquad [15]$$

If we let $W = 100^{\#}$ be the reference weight and let $W_2 = W$, $R_2 = R$ be the charge weight and distance, then

$$(R_{100}/R) \approx (100/W)^{.5} \qquad [16]$$

or

$$(R_{100}/R) \approx 10\, W^{-.5} \qquad [17]$$

This relation is very close to the one given by Johnson.[3] It just varies in the constant and the power of $W$. If we had used more accurate values for $\bar{\alpha}$ and $\bar{\beta}$ we would have obtained values even closer to Johnson's. In principle it is seen that by starting with the energy concept of iso-damage we end up with the Johnson Blast Relationship.[3]

C. More accurate* formulation of iso-damage curves for blasts at a distance from the target

Brode[6-8] obtained the pressure time relation for spherical blast waves as well as impulse values for the positive phase of the explosion. As pointed out in an earlier reference[9] the maximum underpressure in the negative phase of the pressure is generally much smaller than the peak overpressure at the shock front so that less plastic damage will occur in the negative phase than in the positive phase. We will therefore use the positive phase impulse and energy values to determine the damage. Further study of the effect of the negative phase on the plastic deformation of nonlinear structures will certainly be warranted at a future date.

Although Brode's values of pressure and positive duration are slightly in error (as compared with experiment[10]) for spherical pentolite with values of $R/W^{1/3}$ greater than 20 ($R$ being the distance of target to explosion and $W$ being the weight of explosive) it is still felt that the form of the pressure time history in the positive phase is given accurately by Brode and therefore his impulse values will be satisfactory. The impulse and energy that will be used to describe the iso-damage curves are the positive duration values. Thus

$$I = \int_0^T P(t)\, dt \qquad [18]$$

and

$$E_f = \frac{1}{\rho_0 c_0} \int_0^T p^2(t)\, dt \qquad [19]$$

where T is the positive duration of the overpressure.

---

* i.e. More accurate than the theory: - Ref. 1

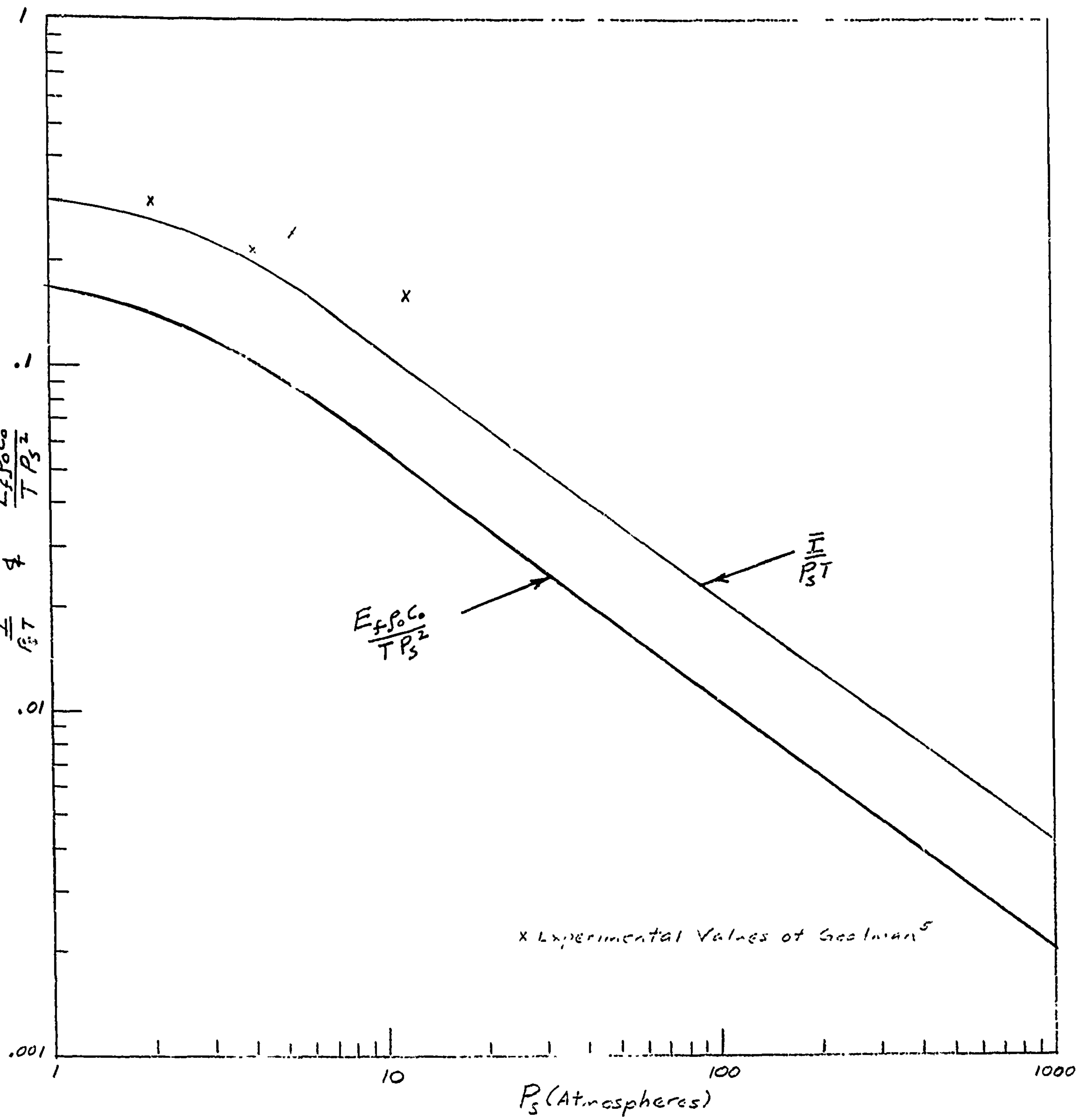


Fig. 3 Nondimensional Impulse and Energy Values

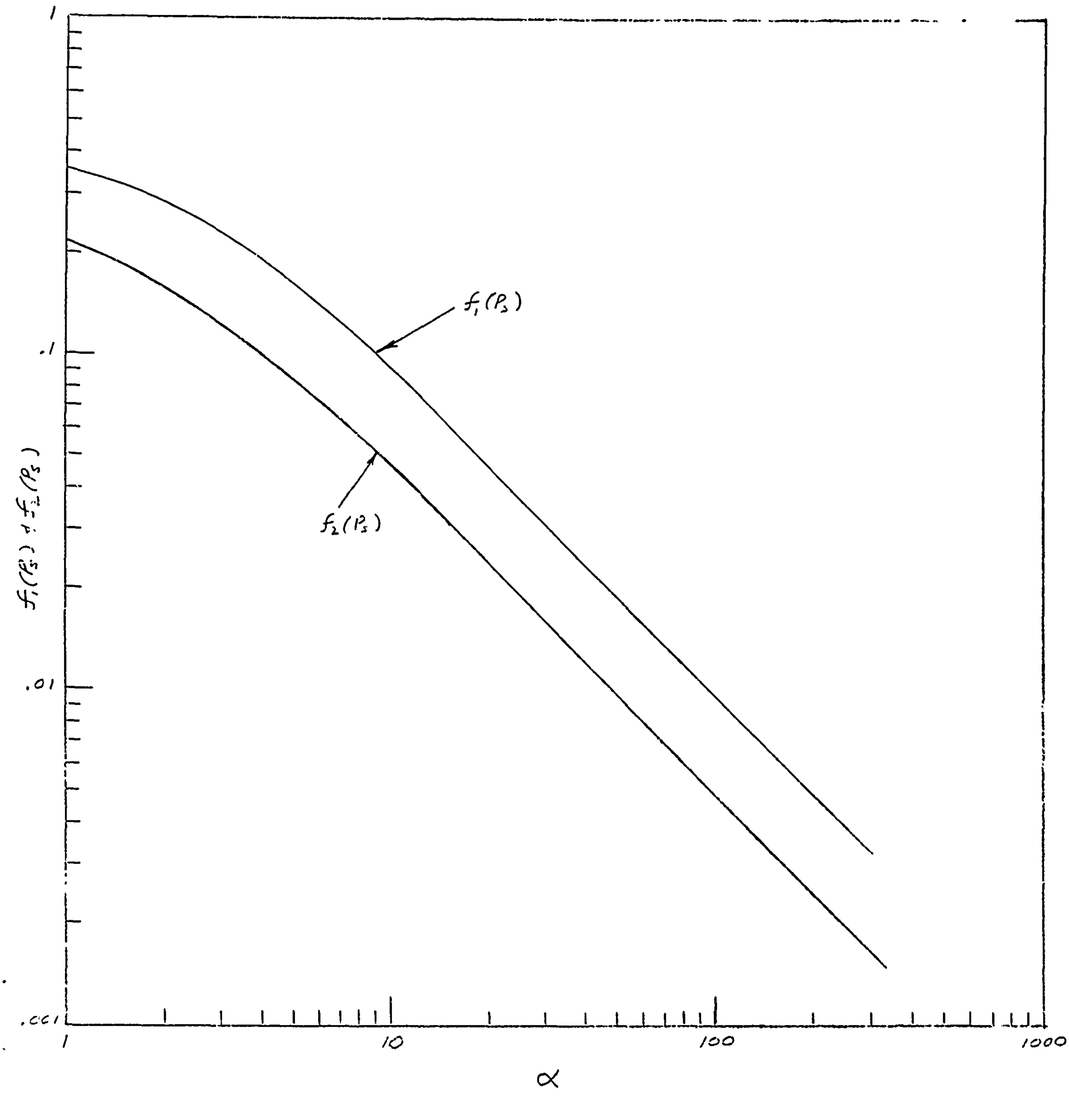


Fig. 4 Nondimensional Impulse and Energy as a Function of Time Constant of Decay

Let $$z = t/T \qquad [20]$$

then $$I = T\int_0^1 P(z)\,dz \qquad [21]$$

and $$E_f = \frac{T}{\rho_0 c_0}\int_0^1 P^2(z)\,dz \qquad [22]$$

The pressure-time relation during the positive phase can be written in the form [6,11]

$$P(z) = P_s(1-z)\,e^{-\alpha z} \qquad [23]$$

where $\alpha$ is a nondimensional constant which is dependent upon $P_s$, the peak value of overpressure. The impulse and energy can then be written

$$I = P_s T\int_0^1 (1-z)\,e^{-\alpha z}\,dz \qquad [24]$$

$$E_f = \frac{T P_s^2}{\rho_0 c_0}\int_0^1 \left[(1-z)\,e^{-\alpha z}\right]^2 dz \qquad [25]$$

So $$I/P_s T = f_1(P_s) = \int_0^1 (1-z)\,e^{-\alpha z}\,dz \qquad [26]$$

$$E_f\rho_0 c_0/T P_s^2 = f_2(P_s) = \int_0^1 \left[(1-z)\,e^{-\alpha z}\right]^2 dz \qquad [27]$$

where $f_1(P_s)$ and $f_2(P_s)$ are nondimensional impulse and energy functions. Integrating, we obtain

$$f_1(P_s) = \frac{1}{\alpha} - \frac{1}{\alpha^2}\left(1-e^{-\alpha}\right) \qquad [28]$$

$$f_2(P_s) = \frac{1}{2\alpha}\left[1 - \frac{1}{\alpha} + \frac{1}{2\alpha^2}\left(1-e^{-2\alpha}\right)\right] \qquad [29]$$

where the time constant, $\alpha$, is a function of $P_s$. Using the values of impulse, overpressure and positive duration given by Brode [7], a curve of $f_1(P_s)$ as a function of $P_s$ has been obtained and is given in Fig. 3. A few experimental values as given by Goodman[5] are plotted on the curve. For low overpressures the agreement between theory and experiment is satisfactory. However for the higher overpressures (greater than 10 atmospheres) there are too few experimental points and too much scatter to draw any definite conclusions.

The value of $\alpha$ was determined by comparing the values of $I/P_s T$ in Fig. 3 with the value of $f_1(P_s)$ given by [28] which is plotted in Fig. 4. The nondimensional energy value, $f_2(P_s)$, was then obtained from this value of $\alpha$ by using eq. [29]. This nondimensional energy value was then plotted in Fig. 3.

The complete iso-damage curve for any case can then be formulated by eliminating T from equations [26] and [27], i.e.

$$\frac{I}{P_s f_1(P_s)} = \frac{E_f \rho_0 c_0}{f_2(P_s) P_s^2} \qquad [30]$$

So

$$(IP_s)^{f_2(P_s)/f_1(P_s)} = E_f \rho_o c_o \qquad [31]$$

For large values of $P_s$

$$f_1(P_s) \approx \frac{1}{\alpha}\left[1-\frac{1}{\alpha}\right] \qquad [32]$$

$$f_2(P_s) \approx \frac{1}{2\alpha}\left[1-\frac{1}{\alpha}\right]$$

So, for large $P_s$

$$f_1(P_s)/f_2(P_s) \approx \frac{1}{2} \qquad [33]$$

and

$$IP_s \approx 2 E_f \rho_o c_o \qquad [34]$$

Equation [34] is exactly the equation obtained for the simple exponential in Reference 1 and in Section IIA of this report.

D. Short time contact explosions

We understand blast loading as that loading due to a standoff explosion which produces a propagating shock wave in the air. There are other cases of impulse response under explosive loading which do not fall into the category of blast. One example is the case of a contact explosion produced by sprayed explosive.[12] The sprayed explosive models are exposed to very short time loading of various distributions. In order to derive an expression for the response in this case, we start with Hamilton's Principle[13]

$$\delta \int_{t_1}^{t_2} [\bar{T}' - \bar{U}]dt = 0 \qquad [35]$$

where $\bar{T}' = \frac{1}{2}\int_A \mu(\dot{u}^2+\dot{v}^2+\dot{w}^2)dA$, the kinetic energy

$\mu$ = mass per unit area of structure

$dA$ = element of surface area

$\dot{u}, \dot{v}, \dot{w}$ = velocities in the three coordinate directions

Assume that we know the distribution of the displacements from some experimental work, then $u, v, w$ can be written

$$u = u_o(t) f_u(A) \qquad [36]$$
$$v = v_o(t) f_v(A)$$
$$w = w_o(t) f_w(A)$$

where $f_u, f_v, f_w$ are the distributions of $u, v, w$ over the surface of the structure

The variation $\delta$ is taken exactly as in the elastic problem.[13] This problem is equivalent to the following problem in the Calculus of Variations:

Find the functions $y_1(x), y_2(x) \ldots y_n(x)$ which take on given values for $x = a$ and $x = b$ and which minimize the definite integral

$$J = \int_a^b F(x, y_1(x), y_2(x) \cdots y_n(x); y_1'(x), y_2'(x) \cdots y_n'(x))\, dx \qquad [37]$$

The result is that $F$ must satisfy the set of Euler Equations

[38]

In our case $F = \bar{T}' - \bar{U}$

$$y_1 = u_0,\ y_2 = v_0,\ y_3 = w_0,\ y_1' = \dot{u}_0,\ y_2' = \dot{v}_0,\ y_3' = \dot{w}_0 \qquad [39]$$

Thus

$$F = \frac{1}{2}\int_A \mu (\dot{u}^2 + \dot{v}^2 + \dot{w}^2)\, dA \quad - V' + W' \qquad [40]$$

where

$$V' = \int_{\bar{V}'} \left( \int_0^{\bar{e}_i} \sigma_i\, de_i \right) d\bar{V}' \quad \text{(work done by internal forces)} \qquad [41]$$

$$W' = \int_A (Xu + Yv + Zw)\, dA \qquad [42]$$

Thus the governing equations for the unknowns $u_0, v_0, w_0$ are

$$\ddot{u}_0 \int_A \mu f_u^2(A)\, dA + \frac{\partial V'}{\partial u_0} = \int_A X(A,t) f_u(A)\, dA$$

$$\ddot{v}_0 \int_A \mu f_v^2(A)\, dA + \frac{\partial V'}{\partial v_0} = \int_A Y(A,t) f_v(A)\, dA \qquad [43]$$

$$\ddot{w}_0 \int_A \mu f_w^2(A)\, dA + \frac{\partial V'}{\partial w_0} = \int_A Z(A,t) f_w(A)\, dA$$

In the large deflection region $V'$ is a function of powers of $u_0, v_0, w_0$ so that the functions $\frac{\partial V'}{\partial u_0}$, $\frac{\partial V'}{\partial v_0}$, $\frac{\partial V'}{\partial w_0}$ are nonlinear functions of $u_0, v_0, w_0$. The equations [43] are therefore ordinary nonlinear differential equations for $u_0, v_0, w_0$. These equations can be written in the standard single degree of freedom form[14]

$$\bar{M}\ddot{x} + \bar{R}x = \bar{P}(t) \qquad [44]$$

where $\bar{M}$ is the generalized mass, $\bar{R}$ is the generalized resistance and $\bar{P}$ is the generalized force. Assume that $u, v$ are small compared to $w$. For the lateral deflection $w$

$$\bar{M} = \int_A \mu f_w^2(A)\, dA$$

$$\bar{R} = \frac{\partial V}{\partial w_0} \qquad [45]$$

$$\bar{P}(t) = \int_A Z(A,t) f_w(A)\, dA$$

For very short time loading eq. [44] can be simplified considerably.[14] If a dynamic loading $P(t)$ is applied to a dynamic system with one degree of freedom (i.e. a system satisfying eq. [44[ the external work done up to any time t is given by

$$W'(t) = \int_0^{x(t)} \bar{P}(t)\,dx = \int_0^t \bar{P}(t)\,\frac{dx}{dt}\,dt \qquad [46]$$

The velocity $\dot{x}(t)$ is determined by integration of eq. [44]

$$\dot{x}(t) = \frac{1}{\bar{M}} \int_0^t [\bar{P}(t) - \bar{R}(x)]\,dt \qquad [47]$$

Thus

$$W'(t) = \int_0^t \bar{P}(t) \left\{ \frac{1}{\bar{M}} \int_0^t [\bar{P}(t) - \bar{R}(x)]\,dt \right\} dt \qquad [48]$$

If the time it takes to reach a maximum deflection is greater than the duration of the load, T, then eq. [48] need only be integrated up to T. Under these circumstances $\bar{R}(x)$ is small during the application of the load and can therefore be neglected. The work $W'$ therefore becomes:

$$W' = \int_0^T \bar{P}(t) \left[ \frac{1}{\bar{M}} \int_0^t \bar{P}(t)\,dt \right] dt \qquad [49]$$

or

$$W' = \frac{\bar{H}^2}{2\bar{M}} \qquad [50]$$

where $\bar{H} = \int_0^T \bar{P}(t)\,dt$

$\bar{H}$ is the total impulse of the external load. This work, $W'$ done by the external load is equal to the work done by the internal forces, $V'$ in deforming the structure

i.e.

$$V = \frac{\bar{H}^2}{2\bar{M}} \qquad [51]$$

where

$$V = \int_{\bar{V}'} \left( \int_0^{\bar{\epsilon}_i} \sigma_i\,d\epsilon_i \right) d\bar{V}' \qquad [52]$$

$$\bar{H} = \int_A \int_0^T Z(A,t)\, f_w(A)\,dt\,dA$$

$$\bar{M} = \int_A \mu\, f_w^2(A)\,dA$$

E. Calculation of structural energy absorption

The loading has been characterized in the previous sections by the peak overpressure, $P_s$, the positive duration of the overpressure, $T$, and the impulse I. For either blast loading[5-8, 15-17] or impulse loading[10,18] these parameters are measurable. The main question is concerned with what effect the magnitudes of overpressure, duration and impulse have on the damage induced in the structure. The characteristics of the structure were given in the previous sections simply by V, the energy absorbed in deforming the structure.

Suppose there are direct stresses $\sigma_x, \sigma_y, \sigma_z$ and shear stresses $\tau_{xy}, \tau_{xz}, \tau_{yz}$ acting on an elemental volume of the structure as shown in Fig. 5:[19]

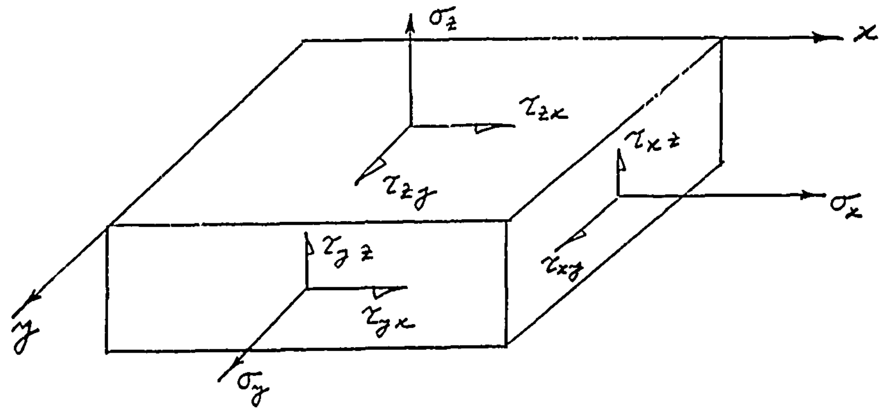


Fig. Free Body Diagram of Elemental Volume

The direct and shear strains are[20] $\epsilon_x, \epsilon_y, \epsilon_z, \gamma_{xy}, \gamma_{xz}, \gamma_{yz}$ . The stress strain curve for one dimensional strain in the $x$ direction will be as shown in Fig. 6:

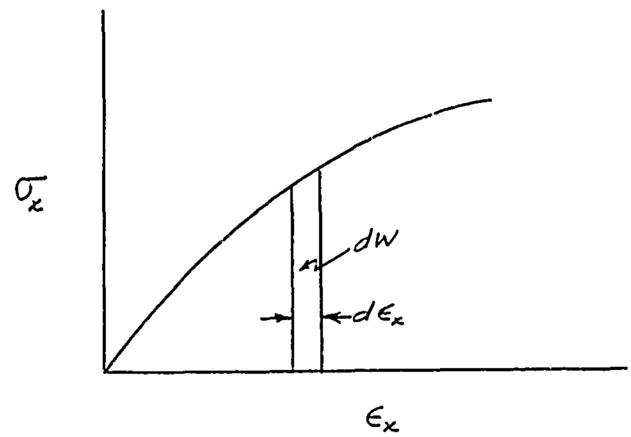


Fig. 6 One Dimensional Stress-Strain Curve

The elemental work for straining in the $x$ direction will then be

$$dw = \sigma_x d\epsilon_x \qquad [53]$$

The total work in direct stress and shear will then be

$$dW = \sigma_x d\epsilon_x + \sigma_y d\epsilon_y + \sigma_z d\epsilon_z + \tau_{xy} d\gamma_{xy} + \tau_{xz} d\gamma_{xz} + \tau_{yz} d\gamma_{yz} \qquad [54]$$

The work per unit volume can be divided into the work done in changing the shape of the body and the work done in changing the volume of the body,[21,22] i.e.

$$w' = 3\int_{\epsilon} \sigma \, d\epsilon + \frac{3}{2}\int_{\gamma_o} \tau_o \, d\gamma_o \qquad [55]$$

in which

$$\sigma = \frac{\sigma_x + \sigma_y + \sigma_z}{3} \quad , \quad d\epsilon = \frac{d\epsilon_x + d\epsilon_y + d\epsilon_z}{3} \qquad [56]$$

and $\tau_o$, $\gamma_o$ are the octahedral shear stress and strain given by[21]

$$\tau_o = \frac{1}{3}\sqrt{(\sigma_x-\sigma_y)^2 + (\sigma_y-\sigma_z)^2 + (\sigma_z-\sigma_x)^2 + 6(\tau_{yz}^2 + \tau_{xz}^2 + \tau_{xy}^2)} \qquad [57]$$

$$d\gamma_o = \frac{2}{3}\sqrt{(d\epsilon_x-d\epsilon_y)^2 + (d\epsilon_y-d\epsilon_z)^2 + (d\epsilon_z-d\epsilon_x)^2 + \frac{3}{2}(d\gamma_{yz}^2 + d\gamma_{zx}^2 + d\gamma_{xy}^2)}$$

If the material is incompressible then the volume does not change and the total work is

$$w' = \frac{3}{2}\int_{\gamma_o} \tau_o \, d\gamma_o \qquad [58]$$

For an incompressible material in a biaxial stress state we replace the octahedral shear stress and strain by their two dimensional counterparts $\sigma_i$ and $e_i$. The work done per unit volume in distortion is then[21,22,23]

$$w' = \int_0^{e_i} \sigma_i \, de_i \qquad [59]$$

where

$$\sigma_i = \sqrt{\sigma_x^2 - \sigma_x\sigma_y + \sigma_y^2 + 3\tau_{xy}^2}$$

$$e_i = \frac{2}{\sqrt{3}}\sqrt{\epsilon_x^2 + \epsilon_x\epsilon_y + \epsilon_y^2 + \frac{1}{4}\gamma_{xy}^2} \qquad [60]$$

The total work done through the entire volume is then

$$V = \int_{\bar{v}'} w' \, d\bar{v}' \qquad [61]$$

The stress-strain law of the material is given by the functional relationship between $\sigma_i$ and $e_i$ as shown in Fig. 7

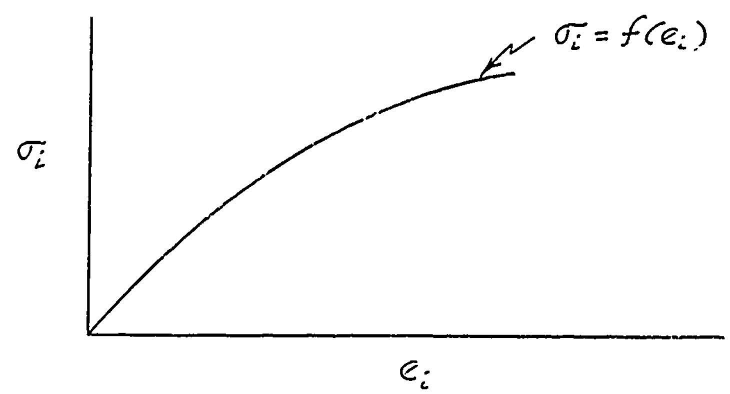


Fig. 7 Form of Stress Strain Law of Material

The stress strain law can have a variety of forms. Most practical cases will fall under the following categories:

1. Rigid-Linear Hardening

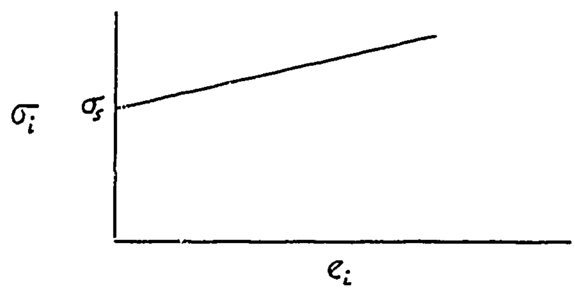


$$\sigma_i = \sigma_s + K e_i$$

$K$ = slope

If $K = 0$ $\sigma_i = \sigma_s$ (perfectly plastic)

Fig. 8 Rigid-Linear Hardening Law

2. Elastic-Linear Hardening

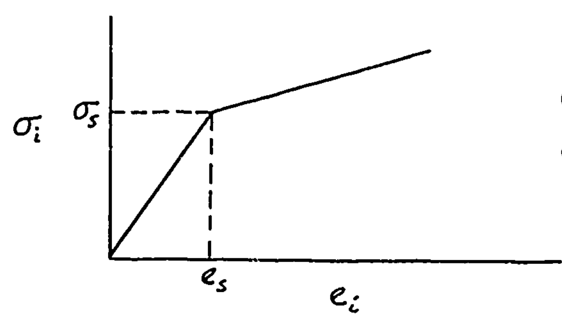


$\sigma_i = E e_i$ for $e_i < e_s$

$\sigma_i = \sigma_s + K(e_i - e_s)$ for $e_i > e_s$

Fig. 9 Elastic-Linear Hardening Law

3. Elastic-Plastic Power Law

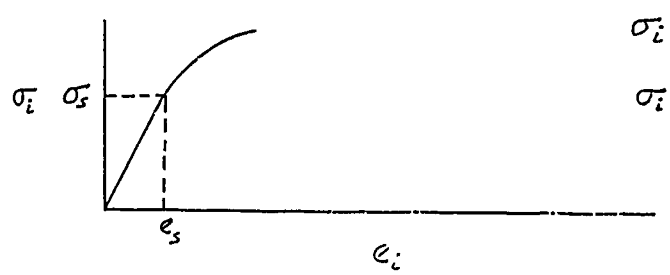


$\sigma_i = E e_i$ for $e_i < e_s$

$\sigma_i = B' e_i^{\bar{p}}$ for $e_i > e_s$

where $B' = \dfrac{\sigma_s}{e_s^{\bar{p}}}$

Fig. 10 Elastic-Plastic Power Law

4. Bell Parabolic Law[24]

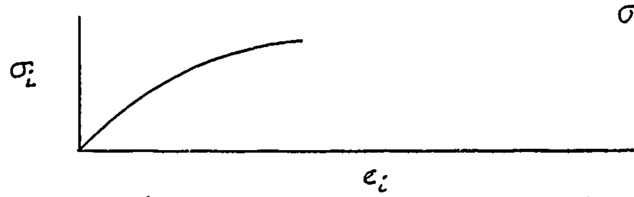


$$\sigma_i = \beta'\left(1 - \frac{T}{T_m}\right)\sqrt{e_i}$$

$T$ = absolute temperature

$T_m$ = melting temperature of material

$\beta'$ = a Universal constant

Fig. 11 Bell Stress-Strain Law

Using each of these laws, substituting into [50] and integrating, the total energy can be put into the following general form

$$V = \left[\int_{\bar{v}'} \left(C_1 e_i^{Q'} + C_2 e_i^{R'} + C_3 e_s^{T'}\right) d\bar{v}' + C_4 \qquad [62]$$

where

1. Rigid-Linear Hardening

$$Q' = 2 \qquad C_1 = K/2$$
$$R' = 1 \qquad C_2 = \sigma_s \qquad \text{For perfectly plastic } K = 0$$
$$T' = 0 \qquad C_3 = 0$$
$$C_4 = 0$$

2. Elastic-Linear Hardening

$$Q' = 2 \qquad C_1 = K/2$$
$$R' = 1 \qquad C_2 = \sigma_s - K e_s$$
$$T' = 0 \qquad C_3 = 0$$
$$C_4 = \frac{K-E}{2} A h e_s^2$$

where A = surface area of the shell

$h$ = shell thickness

3. Elastic-Plastic Power Law

$$Q' = p+1 \qquad C_1 = \frac{\beta'}{p+1}$$
$$R' = 0 \qquad C_2 = 0$$
$$T' = p+1 \qquad C_3 = -\frac{\beta'}{p+1}$$
$$C_4 = \frac{E}{2} A h e_s^2$$

4. Bell Law

$$Q' = 3/2 \qquad C_1 = \frac{2}{3}\beta'\left(1 - \frac{T}{T_m}\right)$$
$$R' = 0 \qquad C_2 - 0$$
$$T' = 0 \qquad C_3 = 0$$
$$C_4 = 0$$

For very large plastic deformations the elastic strains are very small compared to the plastic strains and usually $C_4$ can be placed equal to 0. The energy integral [62] is given in terms of $e_i$ , which is a function of $\epsilon_x, \epsilon_y, \gamma_{xy}$ . The next sections of the report will be devoted to the calculation of this energy for particular structures.

III. Energy absorption curves for various failure shapes of cylindrical shells

A. General relations for energy absorption of cylindrical shells

The strains $\epsilon_x, \epsilon_y, \gamma_{xy}$ of the biaxial stress field can be written[25]

$$\epsilon_x = \epsilon_1 - z\kappa_1 \quad , \qquad \epsilon_y = \epsilon_2 - z\kappa_2 \quad , \qquad \gamma_{xy} = \gamma - 2z\tau \qquad [63]$$

where $\epsilon_1, \epsilon_2, \gamma$ are the midsurface strains, $z$ is the radial distance from the midsurface to any element as shown in Fig. 12 and $\kappa_1, \kappa_2, \tau$ are the curvatures and twist.

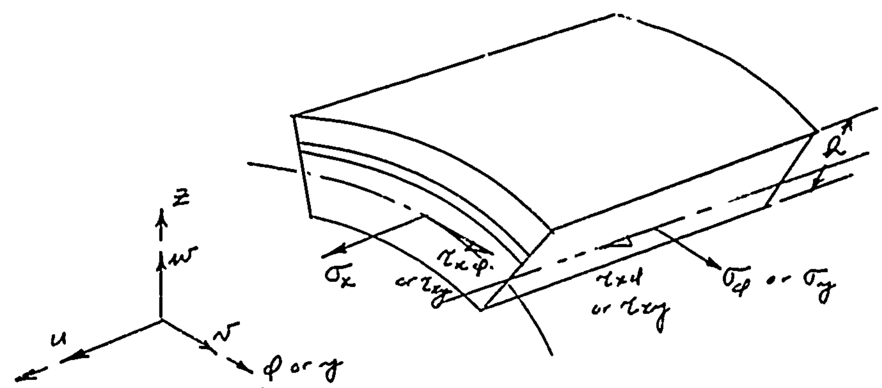


Fig. 12 Stresses on Shell Element

For large deflections the values of $\epsilon_1, \epsilon_2, \gamma$ are[26]

$$\epsilon_1 = \frac{\partial u}{\partial x} + \frac{1}{2}\left(\frac{\partial w}{\partial x}\right)^2 \quad , \qquad \epsilon_2 = \frac{1}{a}\frac{\partial v}{\partial \varphi} - \frac{w}{a} + \frac{1}{2}\left(\frac{\partial w}{a\,\partial \varphi}\right)^2 \qquad [64]$$

$$\gamma = \frac{\partial v}{\partial x} + \frac{1}{a}\frac{\partial u}{\partial \varphi} + \frac{\partial w}{\partial x}\frac{\partial w}{a\,\partial \varphi}$$

The curvatures and twist are[27]

$$\kappa_1 = \frac{\partial^2 w}{\partial x^2} \quad , \qquad \kappa_2 = \frac{1}{a^2}\frac{\partial^2 w}{\partial \varphi^2} + \frac{1}{a^2}\frac{\partial v}{\partial \varphi} \qquad [65]$$

$$\tau = \frac{1}{a}\frac{\partial^2 w}{\partial x\,\partial \varphi} + \frac{1}{a}\frac{\partial v}{\partial x}$$

For very large deformations under intense lateral loading the midsurface strain involving $w$ (i.e. the nonlinear terms) should probably be greater than the linear terms involving $u$ and $v$. Assuming that $u$ and $v$ and their derivatives are much smaller than $w$ and its derivatives, we have

$$\epsilon_x = \frac{1}{2}\left(\frac{\partial w}{\partial x}\right)^2 - z\frac{\partial^2 w}{\partial x^2} \quad , \qquad \epsilon_y = \frac{1}{2}\left(\frac{\partial w}{a\,\partial \varphi}\right)^2 - \frac{w}{a} - \frac{z}{a^2}\frac{\partial^2 w}{\partial \varphi^2} \qquad [66]$$

$$\gamma_{xy} = \frac{\partial w}{\partial x}\frac{\partial w}{a\,\partial \varphi} - 2\frac{z}{a}\frac{\partial^2 w}{\partial x\,\partial \varphi}$$

A large number of practical cases can be fitted to the elastic linear hardening law shown in Fig. 9. Figure 13 shows how an elastic-linear hardening curve can be fitted to an actual stress-strain curve.

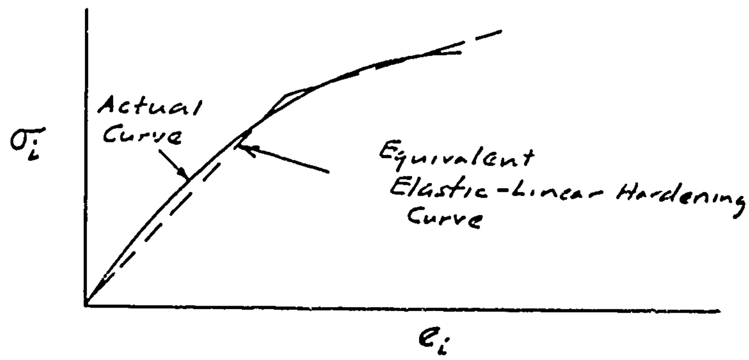


Fig. 13 Fit of Elastic-Linear Hardening Law

Temperature can play an important part in the form of the stress strain law. Figure 14[28] shows the effect of temperature on the yield stress and hardening characteristics of a typical elastic-linear hardening curve.

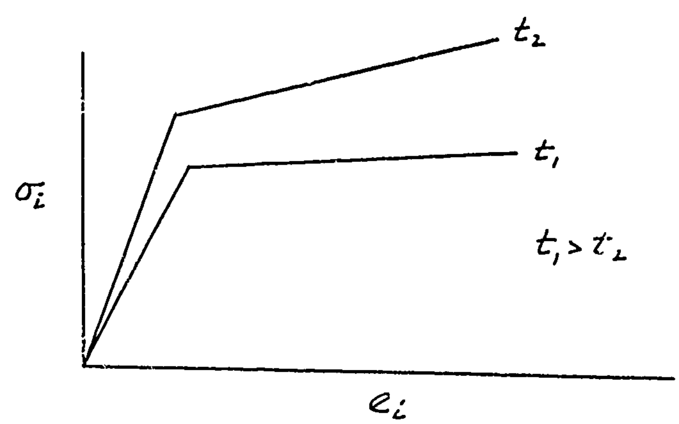


Fig. 14 Effect of Temperature on Stress-Strain Law

The effect of increasing temper-ture is to decrease the yield stress and decrease the hardening.

Since the elastic-linear hardening curve can be used to describe most of the critical characteristics of the metal, we will limit the analysis to this type of stress-strain curve. Under these circumstances the energy absorbed in a cylindrical shell can be written[29]

$$V = \int_0^{\ell}\int_0^{2\pi}\int_{-h/2}^{h/2}\Big[E(1-\lambda)\tfrac{2}{3}\left(\epsilon_x^2+\epsilon_x\epsilon_y+\epsilon_y^2+\tfrac{1}{4}\gamma_{xy}^2\right) + \frac{E\lambda\epsilon_s}{\sqrt{3}}\,2\sqrt{\epsilon_x^2+\epsilon_x\epsilon_y+\epsilon_y^2+\tfrac{1}{4}\gamma_{xy}^2}\,\Big]\,a\,d\phi\,dx\,dz - \frac{E\lambda\epsilon_s^2}{2}\,2\pi a\ell h \qquad [67]$$

where $\lambda = 1 - K/E$ (see Fig. 9)

Substituting the expressions for the strains given by [66], letting $x' = x/\ell$ and $w = w_0 f(x', \varphi)$ and integrating [67], the energy absorbed can be written in the following convenient form:[30]

$$V = \frac{E(1-\lambda)h a \ell}{2(1-\nu^2)} \int_0^1 \int_0^{2\pi} \bar{\alpha}\, dx'\, d\varphi + \frac{E(1-\lambda)}{2(1-\nu^2)} \frac{h}{3} a \ell \int_0^1 \int_0^{2\pi} \bar{\beta}\, dx'\, d\varphi$$
$$+ \frac{\lambda \sigma_s h a \ell}{\sqrt{3}} \int_0^1 \int_0^{2\pi} \left\{ \left[ \frac{(2\bar{\beta}+\bar{\gamma})\sqrt{\bar{\alpha}+\bar{\gamma}+\bar{\beta}}}{4\bar{\beta}} + \frac{(4\bar{\alpha}\bar{\beta}-\bar{\gamma}^2)}{8\bar{\beta}\sqrt{\bar{\beta}}} \sinh^{-1}\left(\frac{2\bar{\beta}+\bar{\gamma}}{\sqrt{4\bar{\alpha}\bar{\beta}-\bar{\gamma}^2}}\right) \right] \right.$$
$$\left. - \left[ \frac{(-2\bar{\beta}+\bar{\gamma})\sqrt{\bar{\alpha}-\bar{\gamma}+\bar{\beta}}}{4\bar{\beta}} + \frac{(4\bar{\alpha}\bar{\beta}-\bar{\gamma}^2)}{8\bar{\beta}\sqrt{\bar{\beta}}} \sinh^{-1}\left(\frac{-2\bar{\beta}+\bar{\gamma}}{\sqrt{4\bar{\alpha}\bar{\beta}-\bar{\gamma}^2}}\right) \right] \right\} dx'\, d\varphi \qquad [68]$$

where

$$\bar{\alpha}(x'; \varphi) = \left(\frac{w_0}{a}\right)^4 \left(\frac{a}{\ell}\right)^4 \frac{1}{4} \left(\frac{\partial f}{\partial x'}\right)^4 + \left(\frac{w_0}{a}\right)^4 \left(\frac{a}{\ell}\right)^2 \frac{1}{2} \left(\frac{\partial f}{\partial x'}\right)^2 \left(\frac{\partial f}{\partial \varphi}\right)^2 - \nu \left(\frac{w_0}{a}\right)^3 \left(\frac{a}{\ell}\right)^2 f \left(\frac{\partial f}{\partial x'}\right)^2$$
$$+ \frac{1}{4}\left(\frac{w_0}{a}\right)^4 \left(\frac{\partial f}{\partial \varphi}\right)^4 - \left(\frac{w_0}{a}\right)^3 f \left(\frac{\partial f}{\partial \varphi}\right)^2 + \left(\frac{w_0}{a}\right)^2 f^2$$

$$\bar{\gamma}(x'; \varphi) = -\left(\frac{w_0}{a}\right)^3 \left(\frac{a}{\ell}\right)^4 \frac{h}{2a} \left(\frac{\partial f}{\partial x'}\right)^2 \left(\frac{\partial^2 f}{\partial x'^2}\right) - \left(\frac{w_0}{a}\right)^3 \frac{h}{2a} \left(\frac{\partial^2 f}{\partial \varphi^2}\right) \left(\frac{\partial f}{\partial \varphi}\right)^2 + 2\left(\frac{w_0}{a}\right)^2 \frac{h}{2a} \frac{\partial^2 f}{\partial \varphi^2} f \qquad [69]$$
$$- \nu \left(\frac{w_0}{a}\right)^3 \left(\frac{a}{\ell}\right)^2 \frac{h}{2a} \left(\frac{\partial f}{\partial x'}\right)^2 \left(\frac{\partial^2 f}{\partial \varphi^2}\right) - \nu \left(\frac{w_0}{a}\right)^3 \left(\frac{a}{\ell}\right)^2 \frac{h}{2a} \left(\frac{\partial^2 f}{\partial x'^2}\right) \left(\frac{\partial f}{\partial \varphi}\right)^2$$
$$+ 2\nu \left(\frac{w_0}{a}\right)^2 \left(\frac{a}{\ell}\right)^2 \frac{h}{2a} f \left(\frac{\partial^2 f}{\partial x'^2}\right) - 2(1-\nu) \left(\frac{w_0}{a}\right)^3 \left(\frac{a}{\ell}\right)^2 \frac{h}{2a} \left(\frac{\partial^2 f}{\partial x' \partial \varphi}\right) \left(\frac{\partial f}{\partial x'}\right) \left(\frac{\partial f}{\partial \varphi}\right)$$

$$\bar{\beta}(x'; \varphi) = \left(\frac{w_0}{a}\right)^2 \left(\frac{a}{\ell}\right)^4 \left(\frac{h}{2a}\right)^2 \left(\frac{\partial^2 f}{\partial x'^2}\right)^2 + 2\nu \left(\frac{w_0}{a}\right)^2 \left(\frac{h}{2a}\right)^2 \left(\frac{a}{\ell}\right)^2 \left(\frac{\partial^2 f}{\partial x'^2}\right) \left(\frac{\partial^2 f}{\partial \varphi^2}\right)$$
$$+ \left(\frac{w_0}{a}\right)^2 \left(\frac{h}{2a}\right)^2 \left(\frac{\partial^2 f}{\partial \varphi^2}\right)^2 + 2(1-\nu) \left(\frac{w_0}{a}\right)^2 \left(\frac{a}{\ell}\right)^2 \left(\frac{h}{2a}\right)^2 \left(\frac{\partial^2 f}{\partial x' \partial \varphi}\right)^2$$

The integrals are dimensionless quantities which are functions of the dimensionless ratios $w_0/a$, $a/\ell$, $h/2a$.

The parameter $\lambda$ and the yield stress $\sigma_s$ are outside the integrals. Therefore the value of the integral is independent of both the hardening and the yield stress.

There are three main types of failure patterns which have been determined experimentally. These typical deformation patterns[15-17] are shown in Figures 15-19. The first two (Figs. 15, 16) are typical patterns associated with blast waves originating at a distance from the shell. The other figures (i.e. Figs. 17-19) are typical patterns from contact explosions[12,18] in the form of a sheet of explosive on the surface of the shell. The analytical functions describing each of these types of patterns and the corresponding energy absorbed will be treated in the next several sections of the report.

B. The single diamond pattern and the lobar buckling pattern

1. Criterion for determining the pattern

In previous work[31] a criterion was determined to establish whether the hinged single diamond pattern (Fig. 15) or the lobar buckling pattern (Fig. 16) would occur. Over the past several years it has been found that this criterion is not quite accurate enough. Using the same ideas as in the previous work, it will be assumed that the diamond pattern is a collapse mode and that the shell will assume this mode of failure if the yield condition is reached. If the load which produces buckling is less than this yield load, then buckling will occur. In order to calculate the yield or collapse load, it will be assumed that the shell is thin enough to take the total load by membrane action alone. Under these circumstances the stress distribution is easily found.[32]

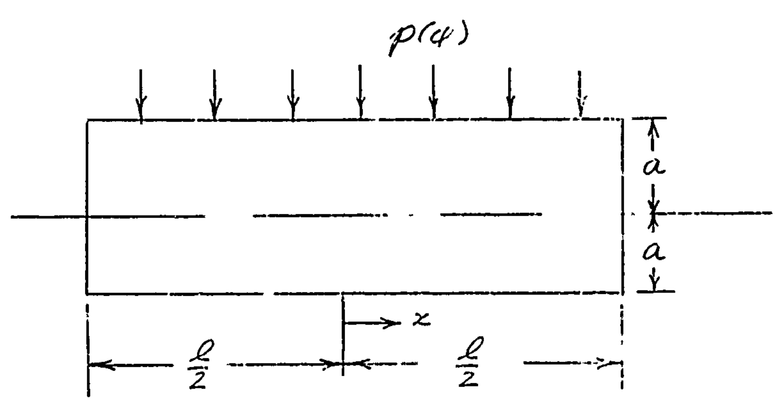


Fig. 20 Statically Loaded Cylindrical Membrane

Let the length of the shell be $\ell$ and assume that it is supported by a diaphragm at each end ( $x = \pm \ell/2$ ). If the origin is at the center of the shell the boundary conditons are

$$N_x = 0 \quad \text{at} \quad x = \pm \ell/2$$

The stress resultants in the shell under a lateral pressure of $p(\varphi)$ are[32]

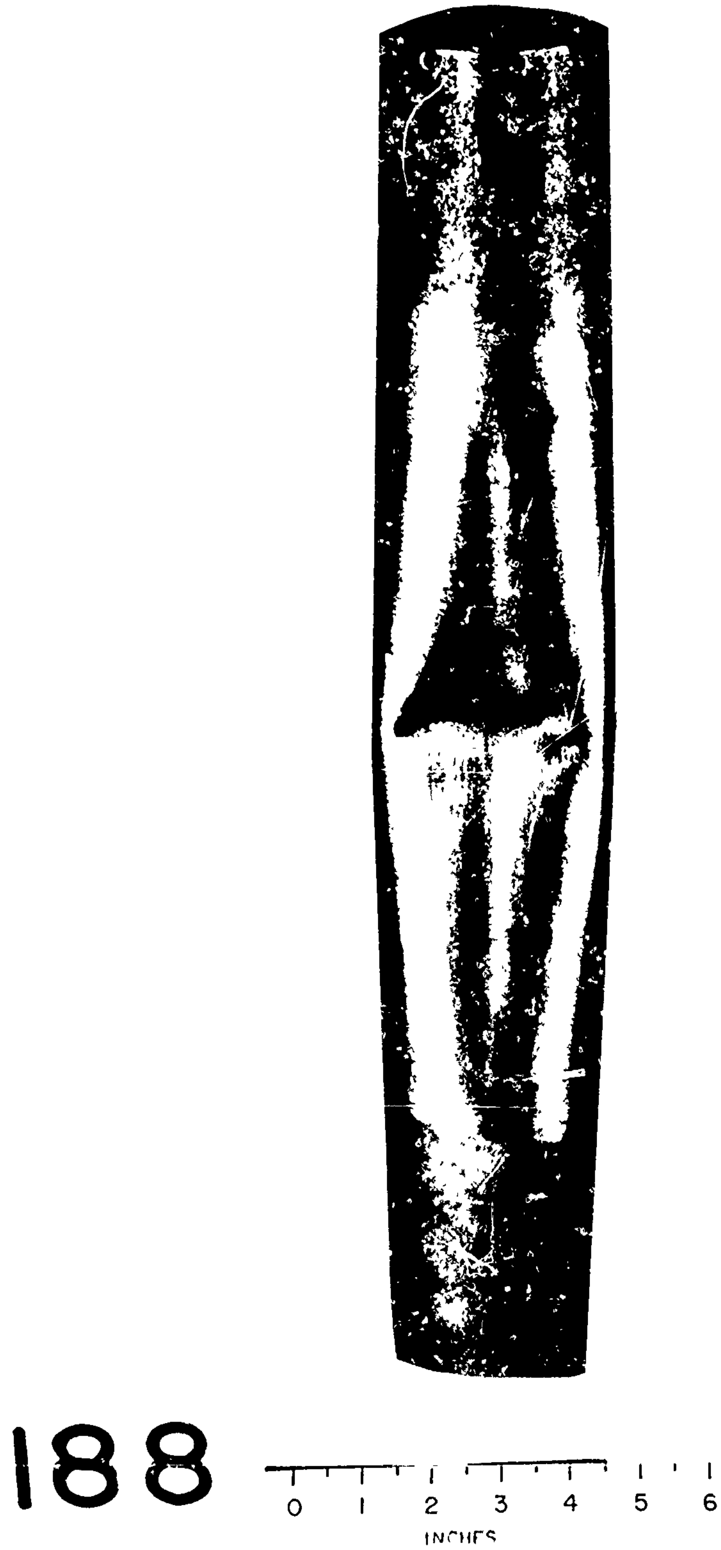


Fig. 15 Collapse Pattern

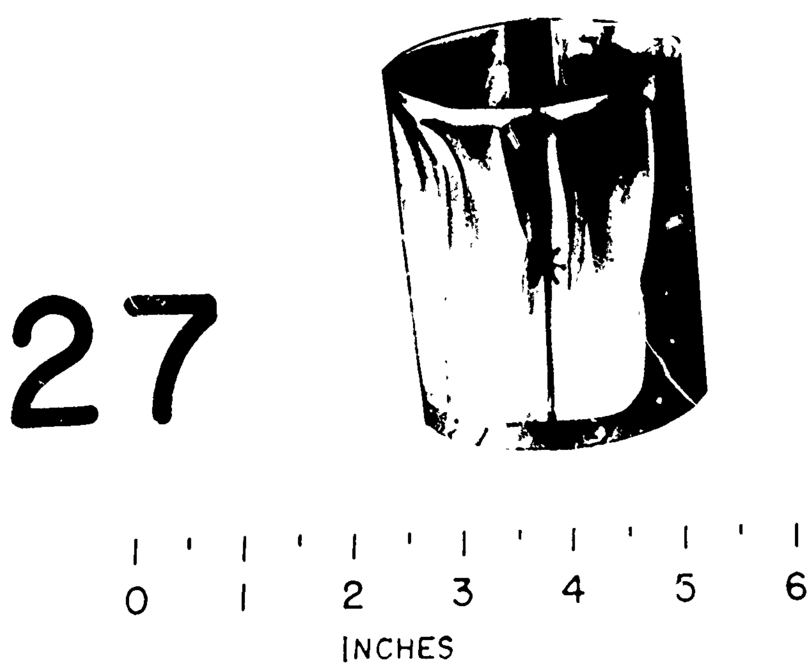


Fig. 16 Buckling Pattern

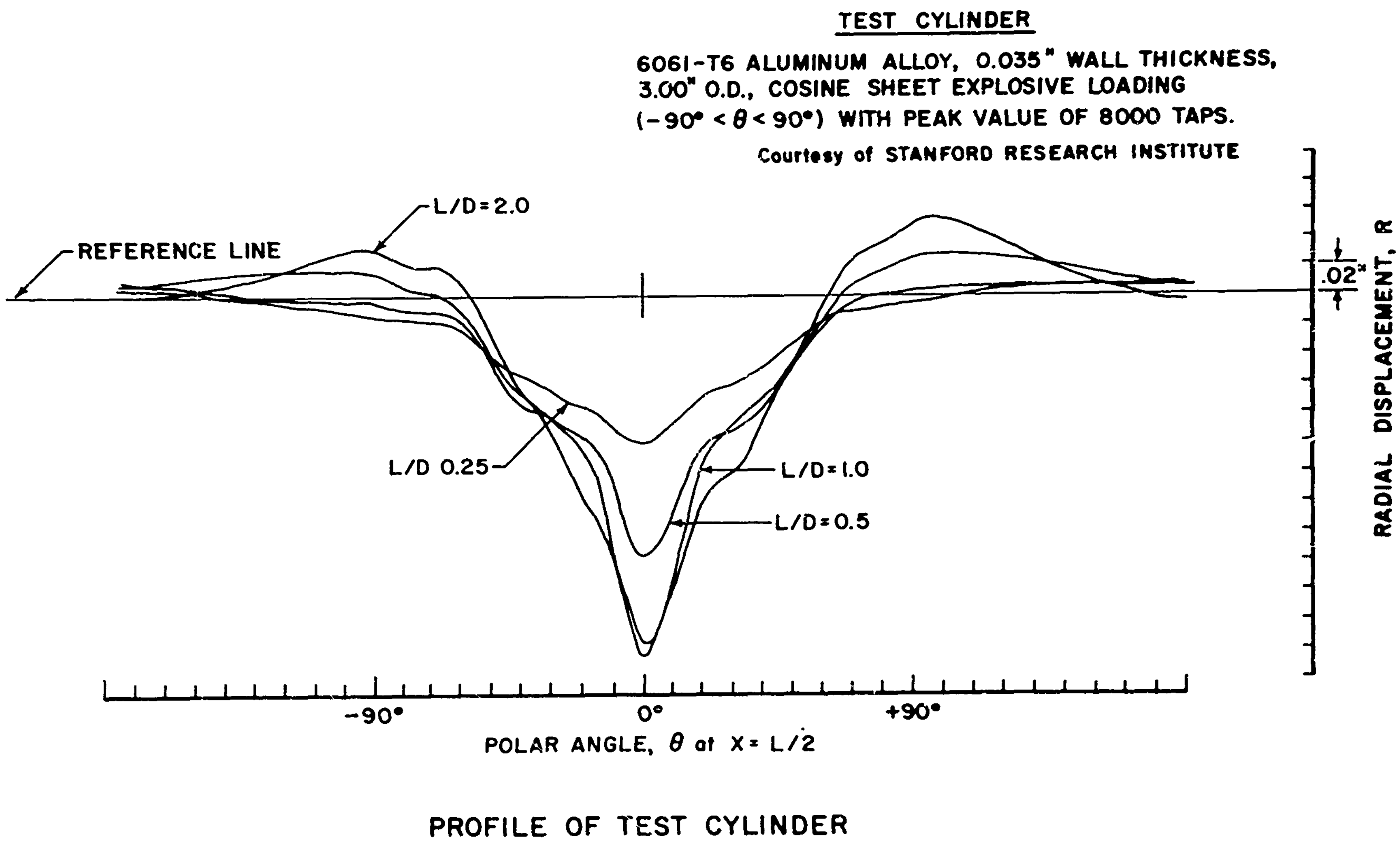


Fig. 17 SRI Peripheral Distribution Patterns

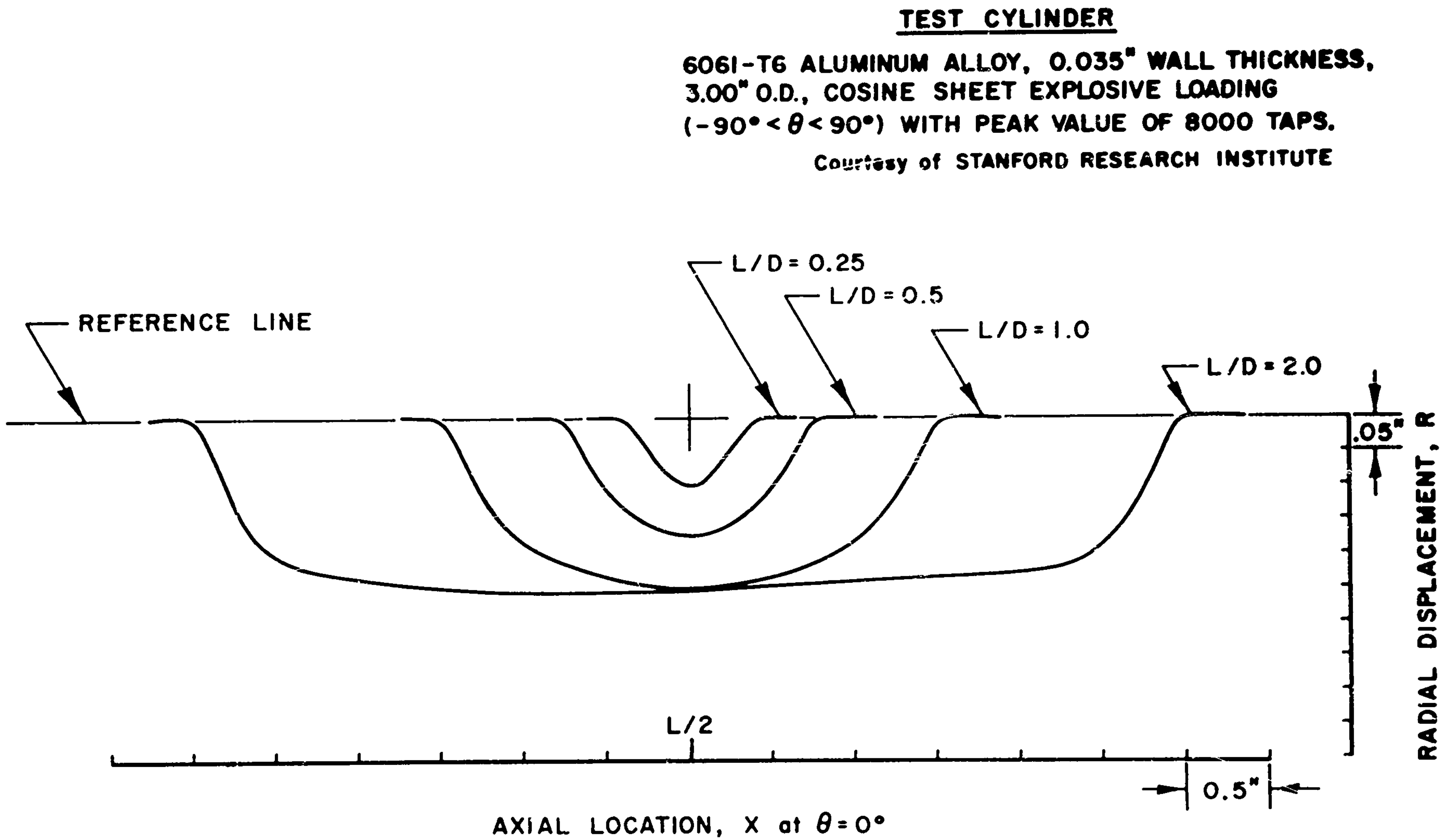


PROFILE OF TEST CYLINDER

Fig. 18 SRI Longitudinal Distribution Patterns

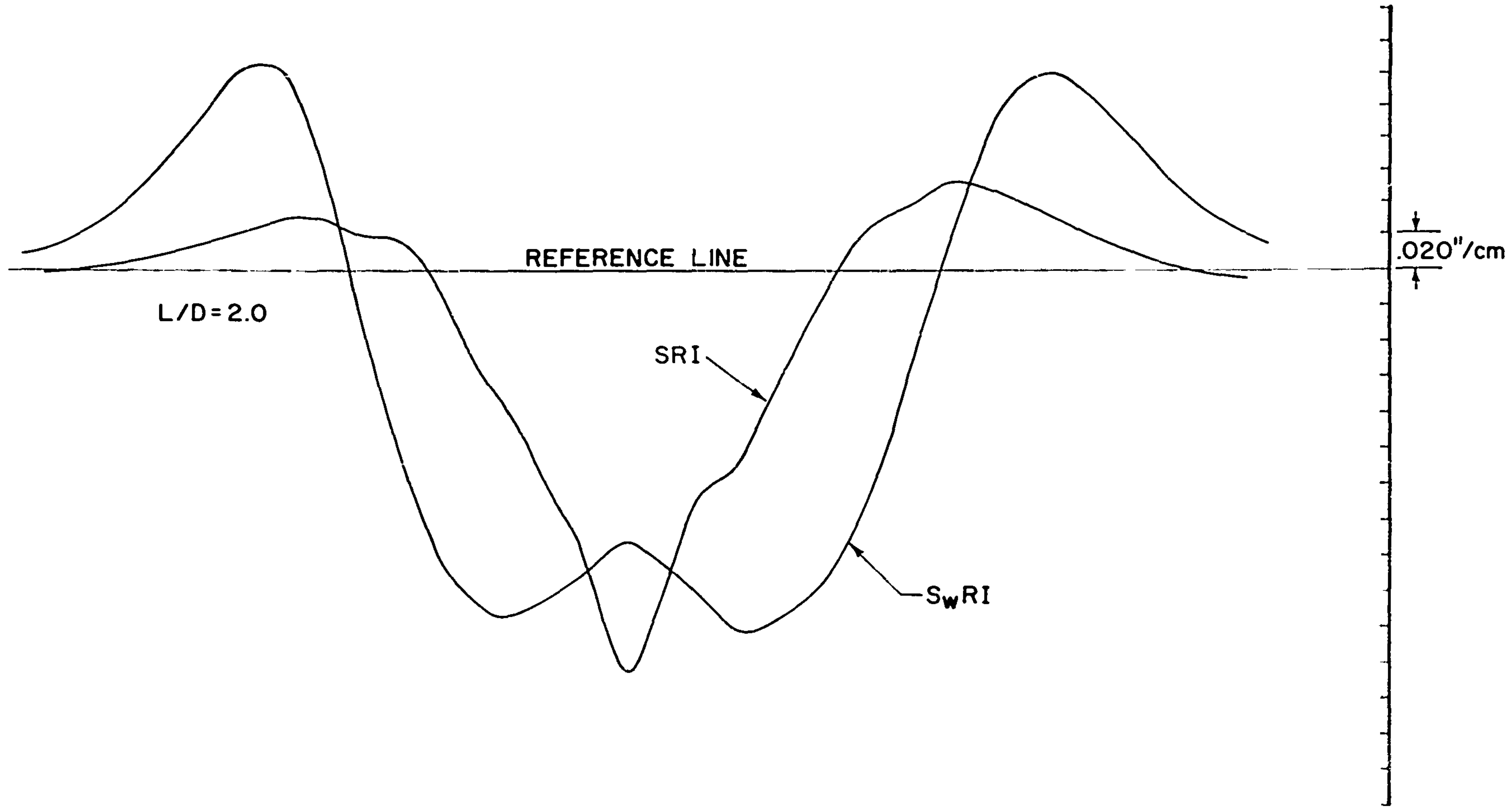


Fig. 19 SRI and $S_w$RI Peripheral Distribution Patterns

$$N_\varphi = a\,p(\varphi)$$
$$N_x = -\frac{1}{8a}(\ell^2 - 4x^2)\frac{dF(\varphi)}{d\varphi}$$
$$N_{x\varphi} = -x\,F(\varphi)$$
$$F(\varphi) = \frac{1}{a}\frac{dN_\varphi}{d\varphi} \qquad [70]$$

At the same time of contact of the shell with the shock wave, the pressure will be a maximum on the side of the shell facing the explosion and decrease to a small value on the back side. The load distribution $p(\varphi)$ will therefore be taken in the following form:

$$p(\varphi) = p_o\,e^{-\alpha'\varphi} \qquad [71]$$

Therefore

$$N_{x\varphi} = x\,p_o\,\alpha' e^{-\alpha'\varphi}$$
$$N_x = -\frac{1}{8a}(\ell^2 - 4x^2)\alpha'^2 p_o\,e^{-\alpha'\varphi} \qquad [72]$$
$$N_\varphi = a\,p_o\,e^{-\alpha'\varphi}$$

A hinge will form at $x = \varphi = 0$ when the yield condition is satisfied at that point, i.e.

$$N_x^2 - N_x N_\varphi + N_\varphi^2 + 3N_{x\varphi}^2 = \sigma_s^2 h^2 \qquad [73]$$

The front face pressure at which yield (or collapse) will start is therefore:

$$p_c = \frac{\sigma_s h}{a}\,\frac{1}{\sqrt{\left(\frac{\ell^2}{8a^2}\alpha'^2\right)^2 + \frac{\ell^2}{8a^2}\alpha'^2 + 1}} \qquad [74]$$

The elastic buckling load for uniform loading of the cylinder is given by Reynolds[33]

$$p_B = \frac{2\pi^2 E f_e}{3\bar{\varphi}(1-\nu^2)}\left(\frac{h}{a}\right)^2 \frac{\left(\frac{\sqrt{ah}}{\ell}\right)^2}{3 - 2\bar{\varphi}(1-f_e)} \qquad [75]$$

where

$$\bar{\varphi} = 1.23\,\frac{\sqrt{ah}}{\ell}$$

$$f_e = \frac{.5}{1 - \dfrac{\left(1-\frac{\nu}{2}\right)\left(\frac{A_f}{\ell h}\right)\left(\beta_e' - \frac{1}{2}\beta_e\right)}{\frac{1}{2}\beta_e\left(\frac{A_f + bh}{\ell h} + 1\right)}}$$

$$\beta_e = \theta_e\left(\frac{\sinh\theta_e + \sin\theta_e}{\cosh\theta_e - \cos\theta_e}\right)$$

$$\beta_e' = \frac{\theta_e}{2}\left(\frac{\sinh\theta_e/2 + \sin\theta_e/2}{\cosh\theta_e/2 - \cos\theta_e/2}\right);\quad \theta_e = [3(1-\nu^2)]^{\frac{1}{4}}\frac{\ell}{\sqrt{ah}}$$

in which $A_f$ is the cross sectional area of the rings which supported the cylinder at $x = \pm\ell/2$ (see Fig. 20), b is the width of the frame in contact with the shell (see Fig. 21)

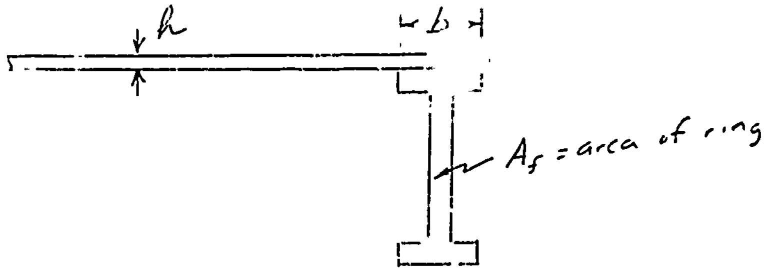


Fig. 21 Cross Section in the Vicinity of the Ring Support

Almroth[34] gives correction curves for buckling under nonuniform loading. The nonuniform peak buckling pressure can be written as $p_B'$ where

$$p_B' = \bar{k}\, p_B \quad , \quad \bar{k} > 1 \qquad [77]$$

2. Comparison of the collapse and buckling relations with experiment

A large number of tests were carried out on shells of various sizes by Schuman.[15-17] The blasts were mostly side on so that the pressure distribution was nonuniform over the shell circumference but uniform over the length. Based upon previous work[35,36] an assumption of $\alpha' = 1$ for calculation of the collapse load seemed reasonable. The buckling load was corrected by use of Almroth's curves.[34] Almroth calculated the buckling pressure of cylinders with the following pressure distribution:

$$p = p_0 + p_1 \cos\varphi \qquad [78]$$

Letting $$\rho' = \frac{p_1}{p_0 + p_1}$$

$$p_1 = \frac{p_0\, \rho'}{1 - \rho'}$$

The peak load is at $\varphi = 0$ and has a value of $(p_0 + p_1)$ .

For our calculations a value of $\rho = .75$ was used to estimate the correction due to nonuniform loading.

The collapse load is then given by

$$\frac{p_c a}{\sigma_0 h} = \frac{1}{\sqrt{\left(\frac{\ell^2}{8a^2}\right)^2 + \frac{\ell^2}{8a^2} + 1}} \qquad [79]$$

and the buckling load by

$$\frac{p_B' a}{\sigma_0 h} = \bar{k}\, \frac{E}{\sigma_0}\; \frac{2\pi^2 f_e \left(\frac{h}{a}\right)}{3\varphi(1-\nu^2)}\; \frac{\left(\frac{\sqrt{ah}}{\ell}\right)^2}{3 - 2\varphi(1-f_e)} \qquad [80]$$

where $E/\sigma_o$ is the ratio of elastic modulus to yield stress and for the test shells is given in a previous reference.[17] $\bar{K}$ is the Almroth correction[34] factor for nonuniform loading. Table 1 gives the results of the theory and experiment. The last two columns indicate whether the shell collapsed or buckled in the tests and what was predicted from the theory. In the theory

$$\text{If } \frac{p_c a}{\sigma_o h} < \frac{p_B' a}{\sigma_o h} \quad \text{Collapse will occur} \qquad [81]$$

$$\text{If } \frac{p_c a}{\sigma_o h} > \frac{p_B' a}{\sigma_o h} \quad \text{Buckling will occur}$$

In Table 1

$$L/D = \ell/2a \;, \quad D/t = 2a/h$$

Table 1 Collapse and Buckling Parameters

| $L/D$ | $D/t$ | Material | $E/\sigma_o$ | $\bar{K}$ | $\frac{p_c a}{\sigma_o h}$ | $\frac{p_B' a}{\sigma_o h}$ | B-Buckling C-Collapse Theor. | Exper. |
|---|---|---|---|---|---|---|---|---|
| 2 | 158 | 1040 Steel | 1000 | 1.25 | .38 | .44 | C | C |
| 2.87 | 158 | | | 1.25 | .21 | .31 | C | C |
| 3 | 158 | | | 1.25 | .20 | .29 | C | C |
| 3.87 | 158 | | | 1.30 | .12 | .23 | C | C |
| 4.87 | 158 | | | 1.35 | .08 | .19 | C | C |
| 6 | 158 | | | 1.40 | .05 | .16 | C | C |
| 8 | 158 | | | 1.50 | .03 | .13 | C | C |
| 2.87 | 86 | | | 1.55 | .21 | .95 | C | C |
| 3 | 86 | | | 1.55 | .19 | .91 | C | C |
| 6 | 86 | | | 1.60 | .05 | .47 | C | C |
| 3 | 316 | | | 1.50 | .19 | .12 | B | not clear |
| 2.91 | 172 | | | 1.40 | .21 | .30 | C | C |
| 3 | 172 | | | 1.40 | .20 | .29 | C | C |
| 2.91 | 79 | | | 1.50 | .21 | 1.03 | C | C |
| 2.94 | 158 | | | 1.25 | .20 | .30 | C | C |
| 2.94 | 88 | | | 1.40 | .20 | .81 | C | C |
| 1.98 | 176 | | | 1.25 | .38 | .38 | C | not clear |
| 2.0 | 1000 | Al 5052-48 | 333 | 1.15 | .19 | .006 | B | B |
| 3.0 | 1000 | | | 1.15 | .38 | .008 | B | B |
| 5.0 | 1000 | | | 1.20 | .077 | .003 | B | B |
| 3.0 | 500 | | | 1.25 | .20 | .017 | B | B |
| 5 | 500 | | | 1.30 | .077 | .011 | B | B |
| 7.67 | 500 | | | 1.35 | .033 | .007 | B | B |
| 10 | 500 | | | 1.40 | .020 | .006 | B | B |
| 3 | 250 | | | 1.25 | .197 | .005 | B | B |
| 3 | 125 | | | 1.25 | .197 | .139 | B | B |

| $L/D$ | $D/t$ | Material | $E/\sigma_o$ | $\bar{k}$ | $\frac{p_c a}{\sigma_o h}$ | $\frac{p_c' a}{\sigma_o h}$ | B-Buckling C-Collapse Theor. | Exper. |
|---|---|---|---|---|---|---|---|---|
| 3 | 2000 | Al 5052-H8 | 333 | 1.10 | .197 | .0019 | B | B |
| 3 | 1000 | | | 1.15 | .197 | .0056 | B | B |
| 3 | 136 | Al 6061-T6 | 250 | 1.30 | .197 | .095 | B | B |
| 3 | 71 | | | 1.50 | .197 | .293 | C | C |
| 3 | 143 | | | 1.30 | .197 | .088 | B | B |
| .67 | 500 | Al 1100-0 | 2000 | 1.10 | .89 | .42 | B | B |
| 1 | 500 | | | 1.10 | .76 | .28 | B | B |
| 1.67 | 500 | | | 1.10 | .48 | .16 | B | B |
| 2 | 500 | | | 1.20 | .38 | .15 | B | B |
| 3 | 500 | | | 1.25 | .19 | .10 | B | B |
| 4 | 500 | | | 1.30 | .12 | .08 | B | B |
| 5 | 500 | | | 1.35 | .076 | .067 | B | B |
| 7.67 | 500 | | | 1.40 | .033 | .045 | C | not clear |
| 3 | 300 | | | 1.25 | .20 | .22 | C | C |
| .67 | 250 | | | 1.20 | .89 | 1.29 | C | C |
| 1 | 250 | | | 1.20 | .76 | .86 | C | C |
| 3 | 250 | | | 1.25 | .20 | .29 | C | C |
| 1.5 | 1000 | | | 1.15 | .54 | .068 | B | B |
| 1.83 | 1000 | | | 1.20 | .43 | .058 | B | B |
| .67 | 500 | | | 1.15 | .89 | .43 | B | B |
| 1 | 500 | | | 1.10 | .76 | .28 | B | B |

It is seen that with very few exceptions the formulas presented in the previous section accurately predict whether the shell will collapse or buckle.

C. Energy in the diamond collapse pattern

The plastic energy absorbed in the collapse pattern during large deformation was obtained in an earlier report.[31] More complete curves are presented here in Figure 22 as a function of the deflection ratio $w_o/a$ which is a more convenient parameter than the one used for collapse in the earlier work.[31] For the linear hardening curve shown in Fig. 9 (see equation 67 for $\lambda$ ), the total energy can be written as

$$V = \frac{\sigma_s h a l}{\sqrt{3}} \left\{ \frac{\sqrt{3}(1-\lambda)}{2e_s(1-\nu^2)} \bar{I}_1 + \lambda \bar{V}_1 - \lambda\sqrt{3}\,\pi e_s \right\} \qquad [82]$$

In Fig. 22 the nondimensional energy functions $\bar{I}_1$ and $\bar{V}_1$ are plotted for a large range of physical parameters. Note that these functions are independent of $D/t$ and for $L/D > 8$ they are independent of $L/D$ . Collapse involving temperature dependence (see Fig. 14) and other hardening problems can be completely solved by this set of curves since both functions $\bar{I}_1$ and $\bar{V}_1$ are independent of the hardening parameter $\lambda$ .

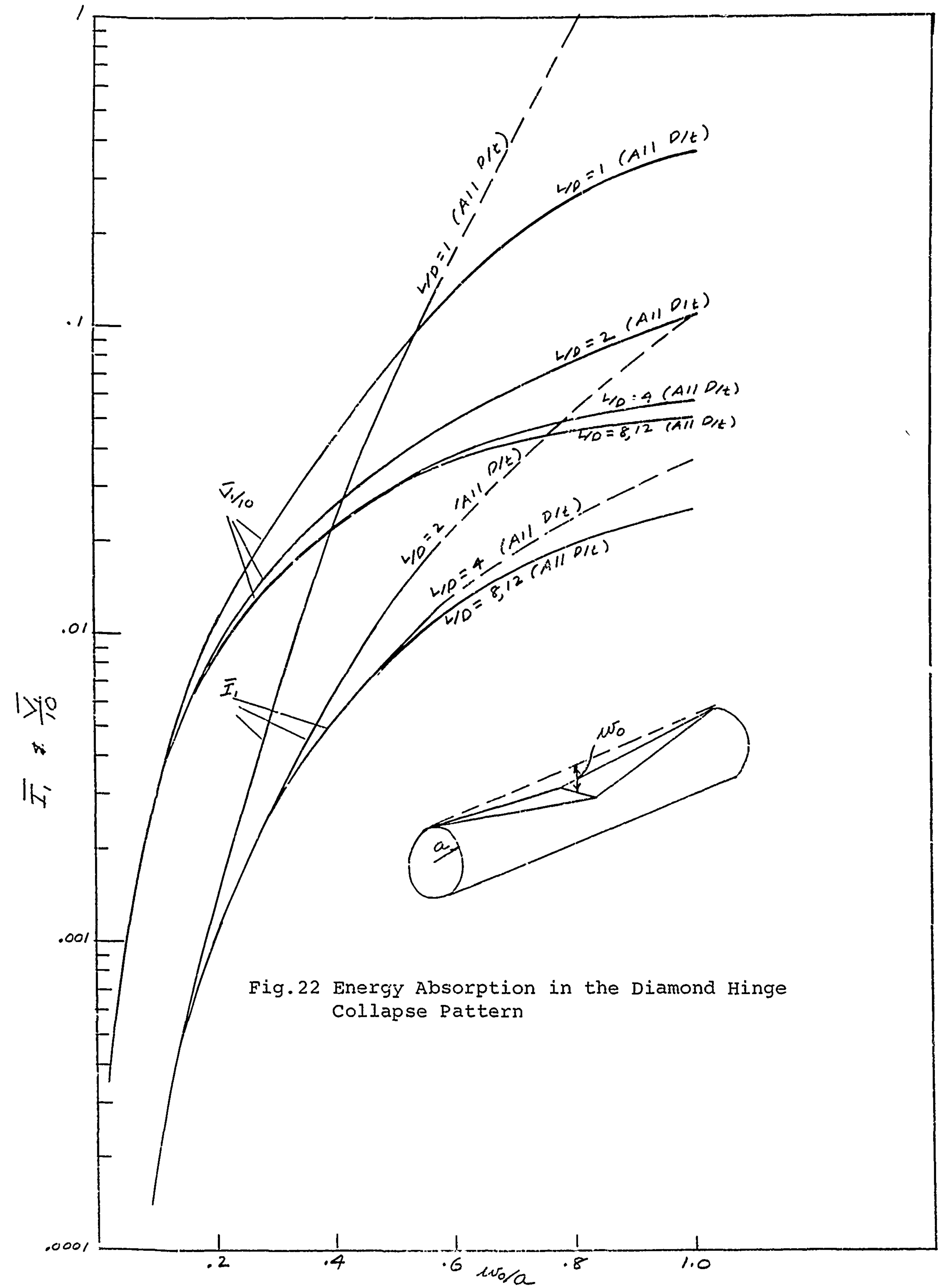


Fig.22 Energy Absorption in the Diamond Hinge Collapse Pattern

## D. Energy in the buckled pattern

A typical buckling pattern that could occur in the shell due to side on blart is shown in Figure 16. The theory predicts one half wave length along the length of the shell and $n$ waves around the periphery, where $n$ is dependent on the geometry of the shell. The manner of buckling is well confirmed by experiment. The displacement pattern in the post failure or plastic region can be described by the following equation:

$$w = w_0 e^{-k\phi} \cos n\phi \qquad [83]$$

The number of peripheral lobes, $n$ is given by Reynold's[33] as

$$n \approx \frac{\pi a}{l} \sqrt{\frac{1}{1.23(\sqrt{al})/l} - 1} \qquad [84]$$

The factor of 1.23 is not exactly correct. Since the number of full waves, $n$, must be a whole number this factor of 1.23 is adjusted so that $n$ is the whole number nearest to the value calculated by using the factor 1.23. The parameter $k$ varies and it is difficult to assign a reliable number to this parameter. Nevertheless a range for can be determined. Based upon examination of experimental result. it seems that $0 < k < 1$ . An extensive set of energy absorption curves for $k = .25$ is shown in Figure 23-25. These curves are based upon the addition of membrane and bending energy. It was found that the membrane was much greated than the bending for buckling in this large deflection region. Figures 26, 27 show a comparison of membrane absorption energies for various values of $k$ between 0 and 1 for several shell geometries. For side on blasts a good average value for $k$ is 25.

## E. Energy in the short duration contact explosion pattern

Some typical deformation patterns for sprayed explosive loading are shown in Figures 17-19. The deformation patterns vary considerably, but all of them can be described by the general form

$$w = w_0 \left[ (1 - e^{-Gx'})^H e^{-C\phi} (1 - B\phi) \frac{\sin K\phi}{K\phi} \right] ; \; x' = x/l \qquad [85]$$

The constants which vary with each pattern are G, H, C, B, K. Figures 28, and 29 show the longitudinal and peripheral displacement distributions for a range of values of these constants. Since the patterns are always symmetrical about $\theta = 0$ and $x' = .5$ only one half of the pattern is shown. The patterns in the Stanford Research Institute tests vary greatly from those in the Southwest Research Institute tests (see Fig. 19). It is therefore difficult to conclude what a typical pattern should be for a given value of $L/D$ and $D/t$ . It is believed that these short duration explosive tests are not as conclusive as the collapse and buckling phenomena from stand off blast as presented earlier in the report.

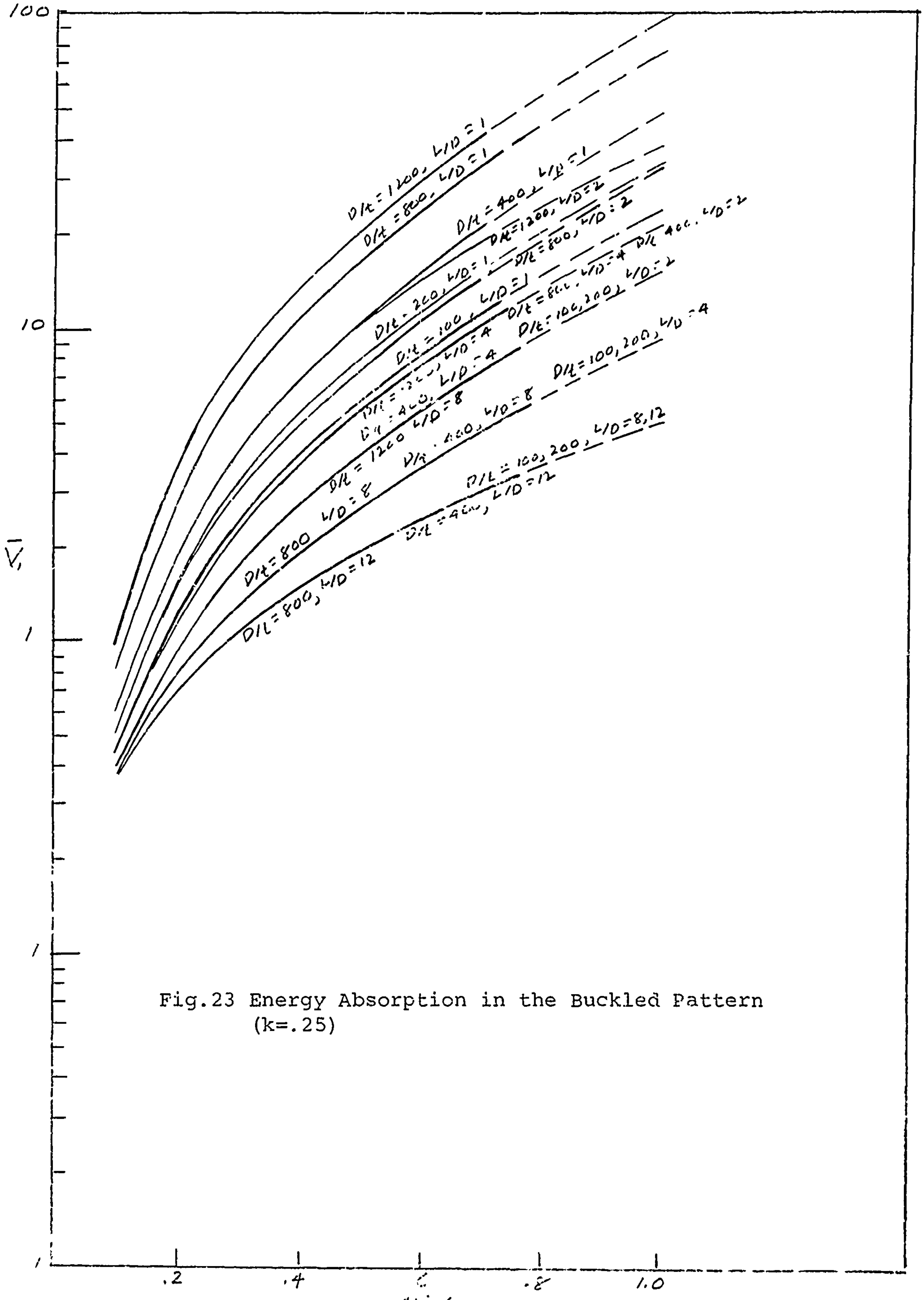

Fig.23 Energy Absorption in the Buckled Pattern (k=.25)

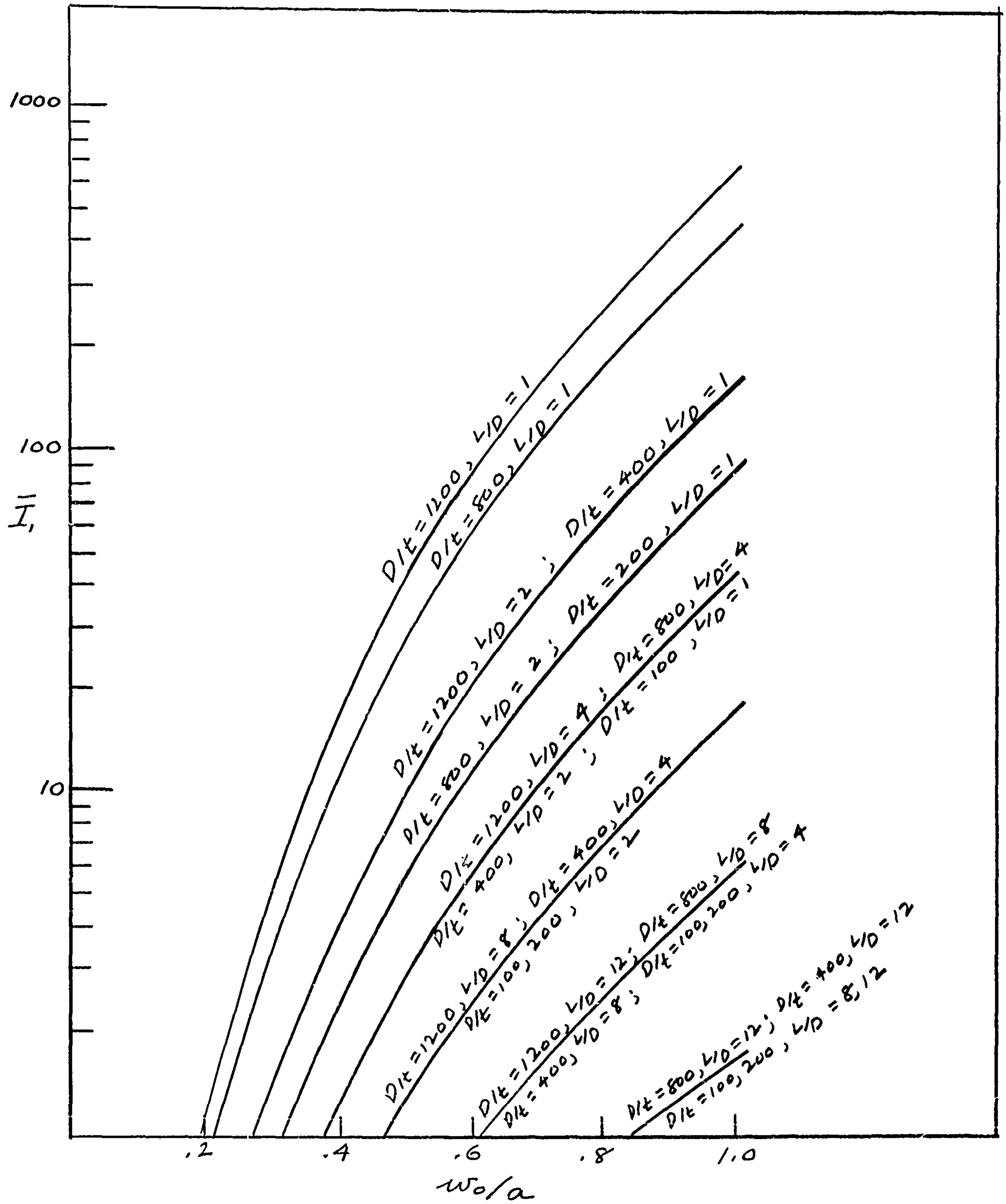


Fig.24 Energy Absorption in the Buckled Pattern
(k=.25)

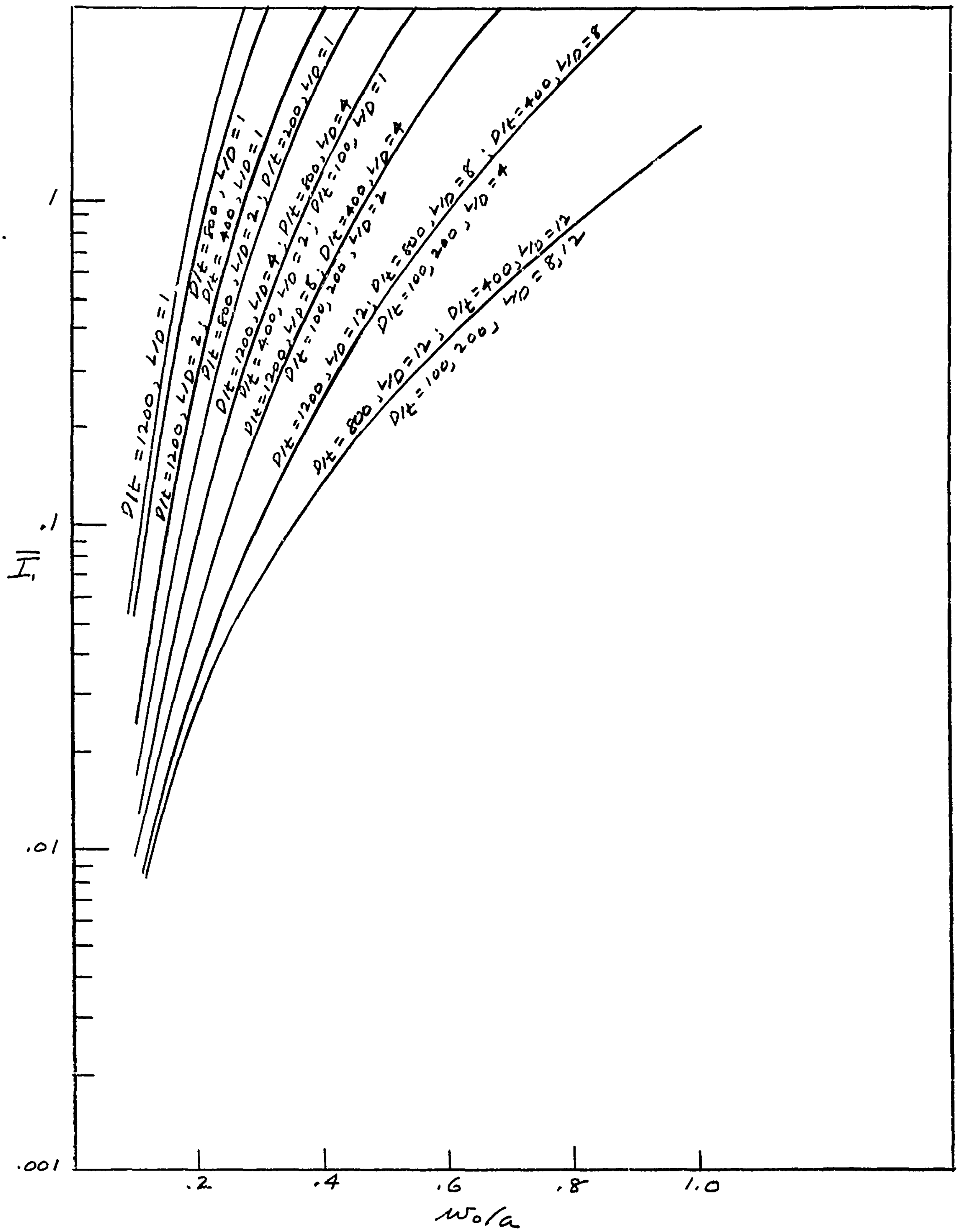


Fig.25 Energy Absorption in the Buckled Pattern
(k=.25)

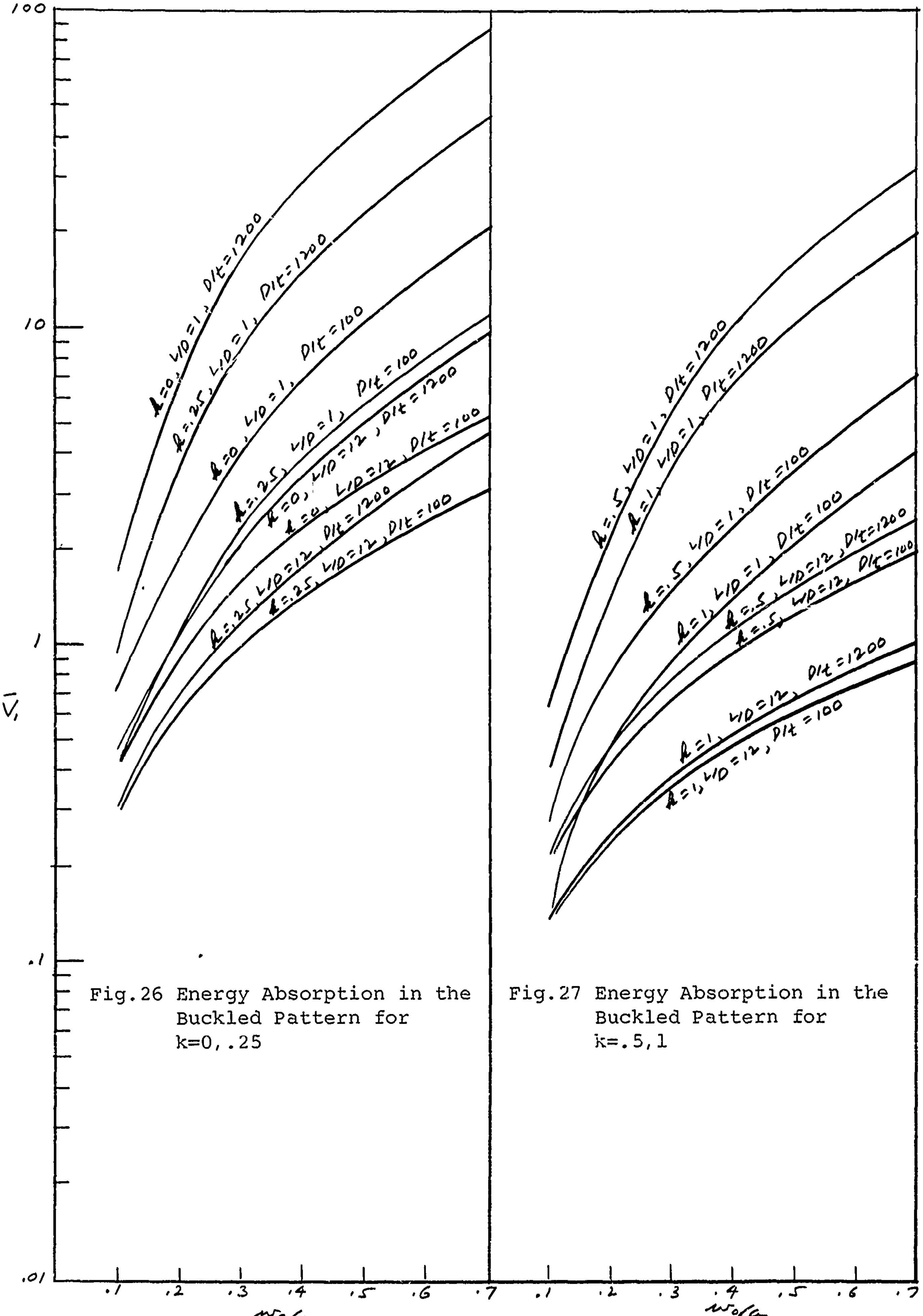


Fig.26 Energy Absorption in the Buckled Pattern for k=0,.25

Fig.27 Energy Absorption in the Buckled Pattern for k=.5,1

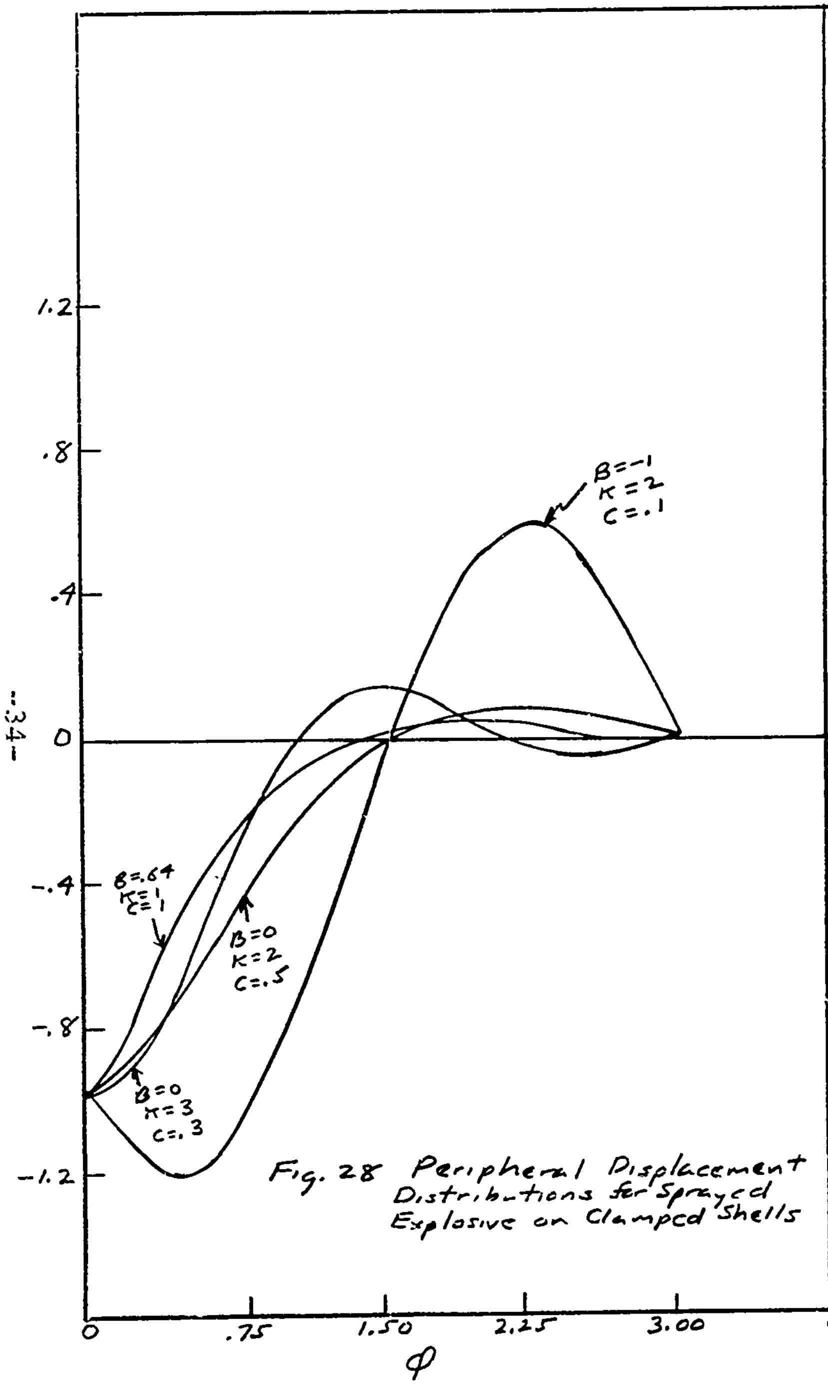


Fig. 28 Peripheral Displacement Distributions for Sprayed Explosive on Clamped Shells

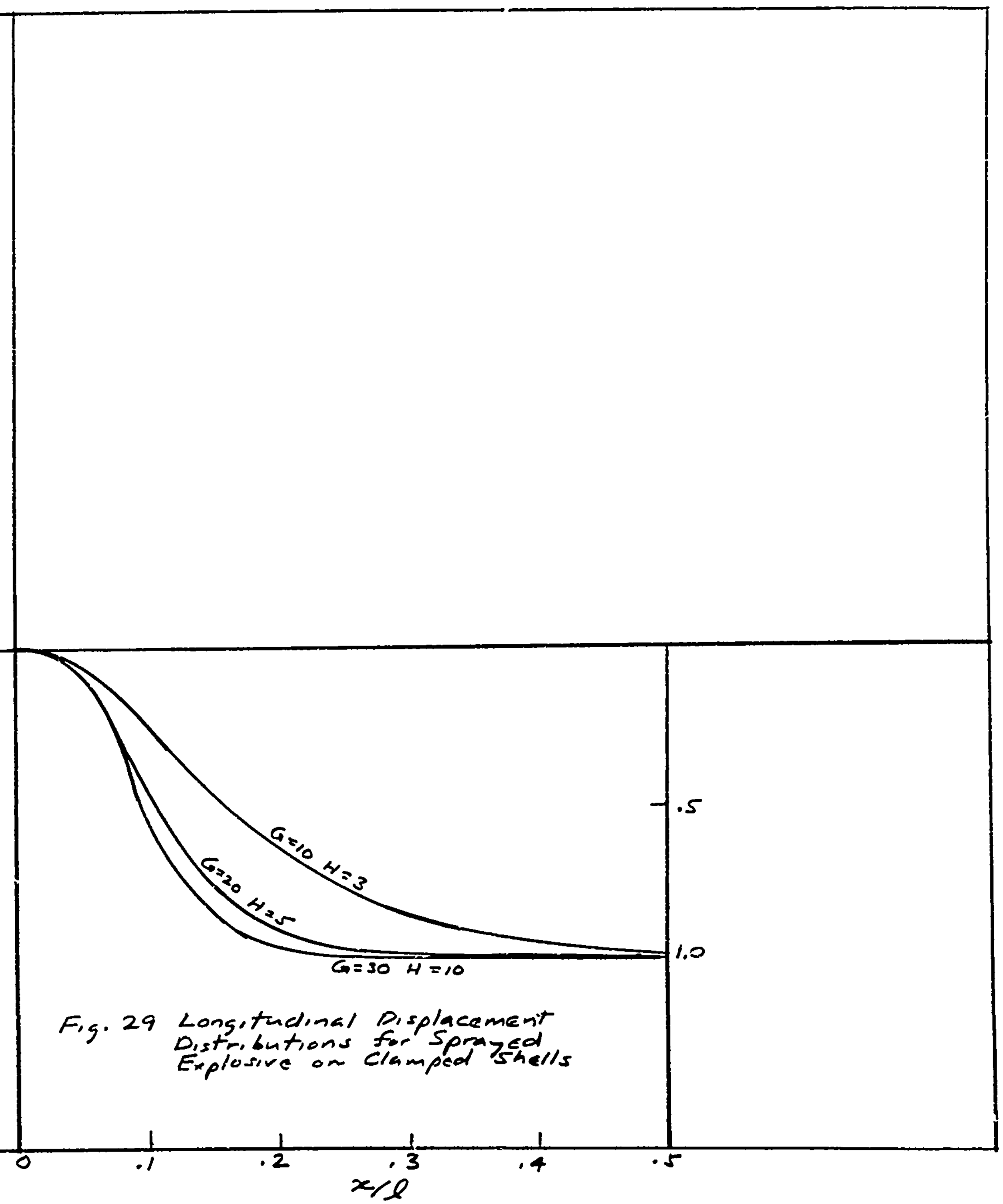


Fig. 29 Longitudinal Displacement Distributions for Sprayed Explosive on Clamped Shells

It was found that the energy of plastic deformation was critically dependent upon the values of the shape parameters G,H,C,B,K. Therefore it would be misleading at this time to tie down energy values as a function of $L/D$, $D/t$. However in the next section of the report the actual impulse values obtained from tests will be compared with those predicted from theory by using representative values of G,H,C,B,K.

## IV. Impulse response of cylindrical shells for short time contact explosions

In Section IIB of this report there is a derivation of the impulse as a function of the energy absorbed. For the cylindrical shell this relation becomes

$$V = W = \frac{\bar{H}^2}{2\bar{M}} \tag{86}$$

where $W = V =$ work done by internal forces (see eq. [68]

$$\bar{H} = \bar{I}\int_0^{\ell}\int_0^{2\pi} f_I(x,\theta)\, f_w(x,\theta)\, a\,dx\,d\theta \tag{87}$$

$$\bar{M} = \mu\int_0^{\ell}\int_0^{2\pi} f_w^2(x,\theta)\, a\,dx\,d\theta$$

where $f_I(x,\theta)$ is the impulse distribution and $\bar{I}$ is the peak value of impulse per unit area. Substituting the value of $V$ from [68], $\bar{H}$ and $\bar{M}$ from [87], we obtain the following relation for a rigid -- perfectly plastic material:

$$\left(\bar{I}/t\sqrt{\rho\sigma_s}\right) = f\left(D/t,\ L/D,\ w_m/a\right) \tag{88}$$

where $f$ is a dimensionless function of the dimensionless parameters $D/t$, $L/D$, $w_m/a$. $\bar{w}_m$ is the maximum deflection, which in all cases considered here, is at $\varphi = 0$, $x = \ell/2$. Equation [88] was programmed on a time sharing system and calculations were run using a cosine distribution of impulse over 180°[12] using representative values of the constants describing the deformation pattern. A rigid perfectly plastic material (see Fig. 8) was assumed. It was found that the following values of the constants gave a deflection distribution which was consistent with the $SRI$ and $S_wRI$ tests (see Fig. 19) and at the same time fitted the damage sensitivity curve of $S_wRI$:[12]

$$B = .64,\ K = 1,\ C = 1,\ G = 10,\ H = 3 \tag{89}$$

The deflection distribution for this set of constants as well as other sets are given in Figures 28, 29. The theoretical curve using the above mentioned constants is compared with the experimental results of Baker, et. al.[12] in Fig. 30. Using the same set of constants curves of the non-dimensional impulse function $\bar{I}/t\sqrt{\rho\sigma_s}$ as a function of $L/D$ and $D/t$ for all values of $w_m/a$ were calculated and plotted in Fig. 31, 32.

The effect of $L/D$ especially for short cylinders in which $L/D < 1$ is very large. For longer cylinders with $L/D > 2$ the effect of $D/t$ is very small. As the $L/D$ decreases the effect of $D/t$ increases. Note that the values of $D/t = 100, 10$ used in Fig. 32 represent a vast range. For $D/t > 100$ there is no effect of $D/t$ whatsoever.

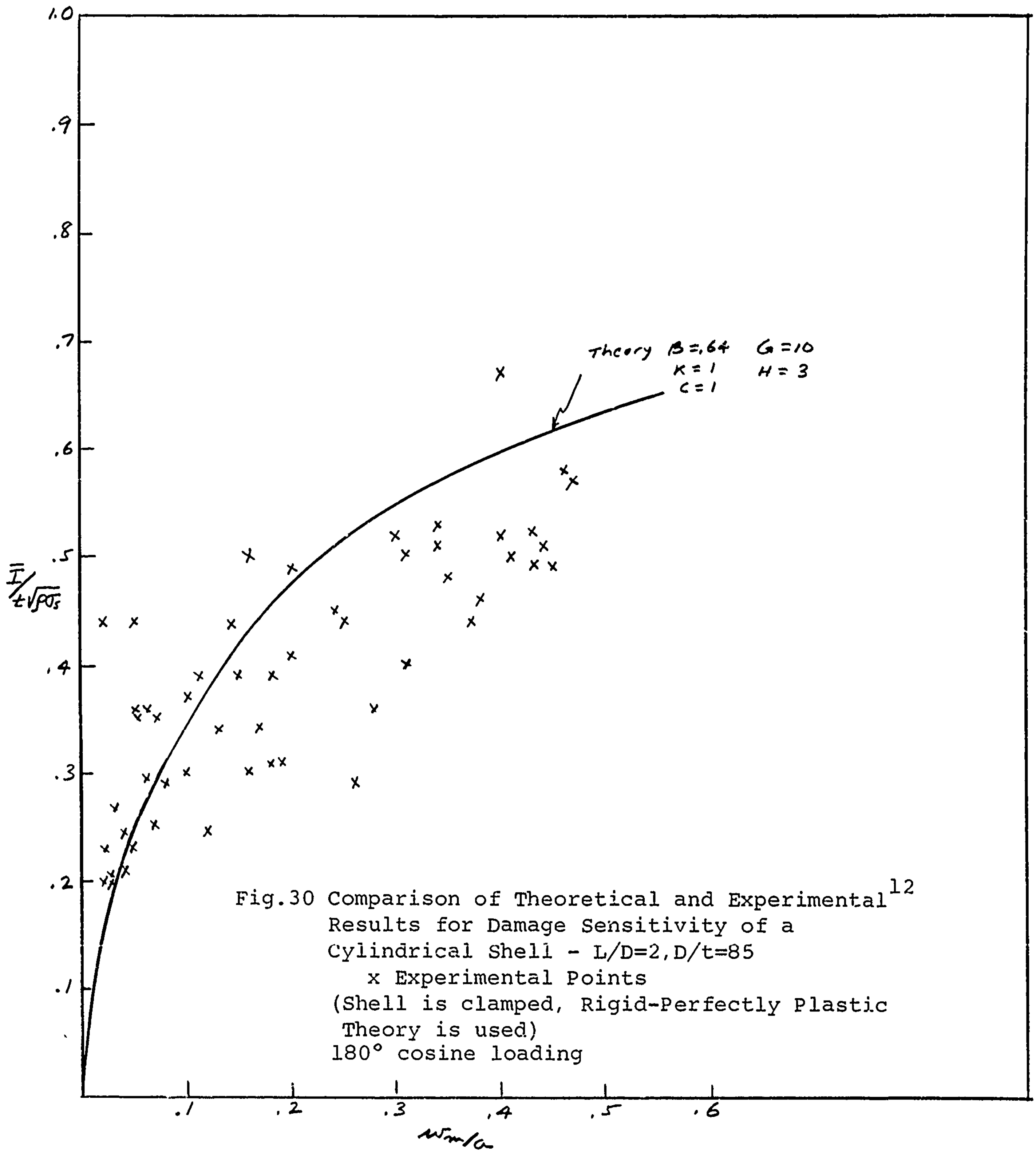


Fig.30 Comparison of Theoretical and Experimental[12]
Results for Damage Sensitivity of a
Cylindrical Shell - L/D=2, D/t=85
x Experimental Points
(Shell is clamped, Rigid-Perfectly Plastic
Theory is used)
180° cosine loading

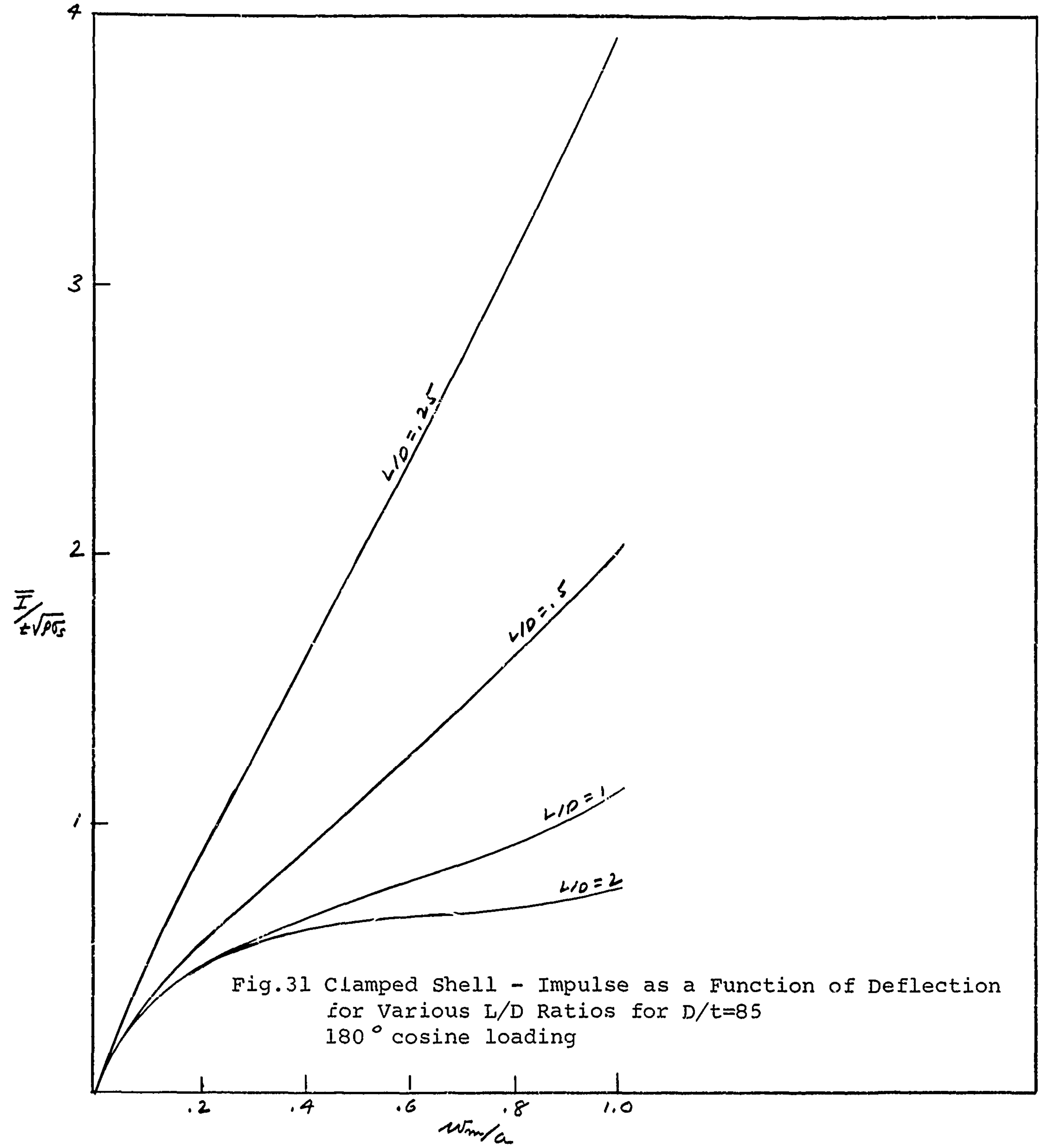


Fig.31 Clamped Shell - Impulse as a Function of Deflection for Various L/D Ratios for D/t=85 180° cosine loading

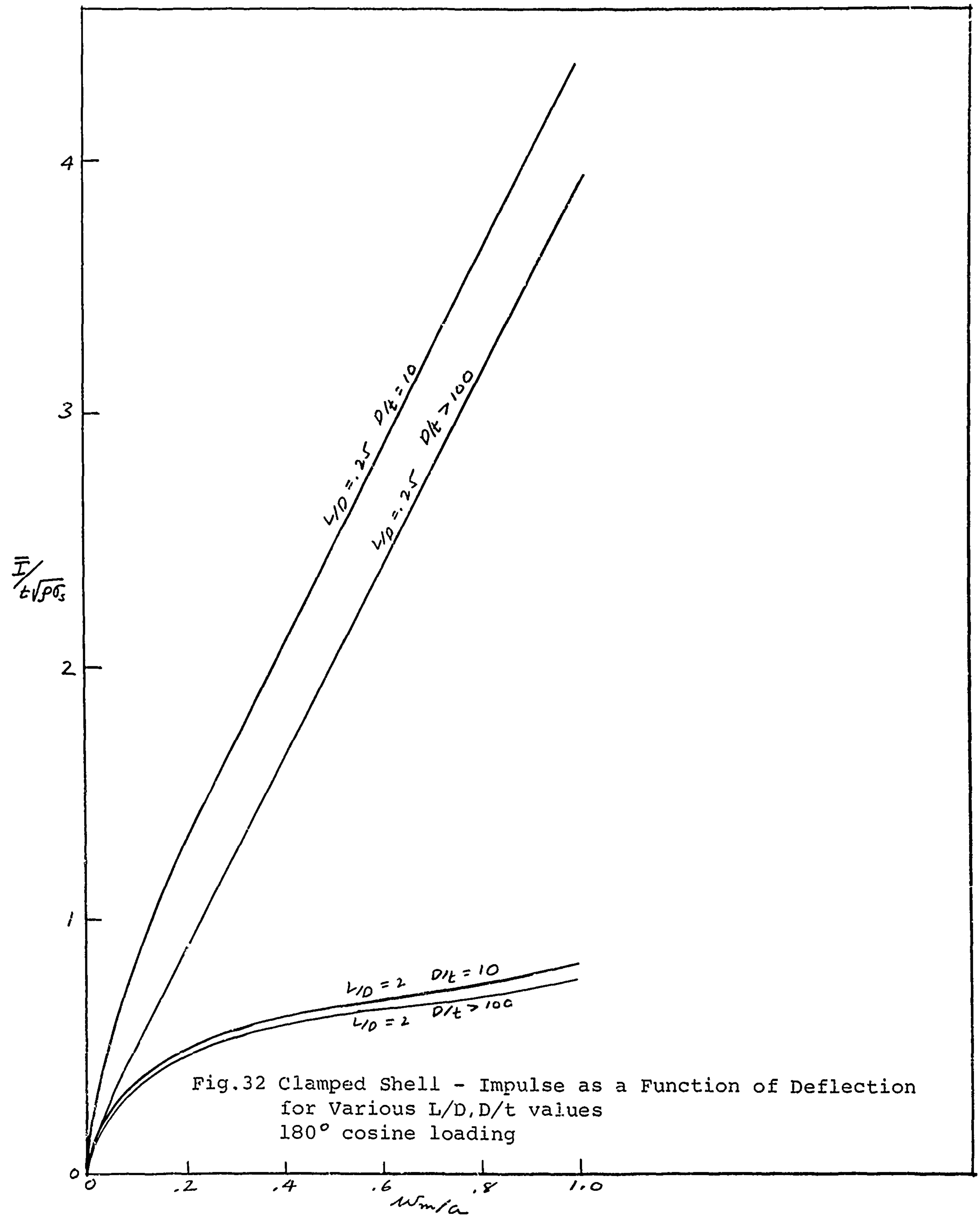


Fig.32 Clamped Shell - Impulse as a Function of Deflection for Various L/D, D/t values
180° cosine loading

## REFERENCES


1. J. E. Greenspon, "Prediction of Iso-Damage Curves," J G Engineering Research Associates, Contract DAAD05-67-C-0331, Tech. Rep. No. 8, July, 1967.
2. R. H. Cole, "Underwater Explosions," Dover Publications, New York, 1965, pp 231-235.
3. O. T. Johnson, "A Blast-Damage Relationship," (Confidential -- Title Unclassified) BRL Report No. 1389, Ballistic Research Laboratories, Aberdeen Proving Ground, Sept. 1967.
4. Ref. 2, p. 241.
5. H. J. Goodman, "Compiled Free-Air Blast Data on Bare Spherical Pentolite," BRL Report No. 1092, Ballistic Research Laboratories, Aberdeen Proving Ground, Feb., 1960.
6. H. L. Brode, "Numerical Solutions of Spherical Blast Waves," Journal of Applied Physics, Vol. 26, No. 6, June 1955, p. 766.
7. H. L. Brode, "Point Source Explosion in Air," Rand Corp., RM-1824-AEC, Dec. 3, 1956, p. 43.
8. H. L. Brode, "The Blast Wave in Air Resulting from a High Temperature, High Pressure Sphere of Air," Rand Corp., RM-1825-AEC, Dec. 3, 1956 (Released 10/30/59).
9. "The Effects of Nuclear Weapons," S. Glasstone, Editor, Superintendent of Documents, U. S. Government Printing Office, April,1962, p.106.
10. W. E. Baker and W. J. Schuman, Jr., "Air Blast Data for Correlation with Correlation with Moving Airfoil Tests," BRL Tech. Note 1421, Ballistic Research Laboratories, Aberdeen Proving Ground, August, 1961.
11. G. F. Kinney, "Explosive Shocks in Air," The MacMillan Co., New York, 1962, Chap. 5.
12. W. E. Baker, S. Silverman, F. O. Hoese, "Impulsive Loading of Simple and Composite Cylinders," Southwest Research Institute, Contract No. DAAD 05-67-C-0160, Feb., 1969.
13. A. E. H. Love, "Mathematical Theory of Elasticity," Fourth Edition, Dover Publications, New York, 1944, p. 166.
14. C. H. Norris, R. J. Hansen, M. J. Holley, J. M. Biggs, S. Namyet, J. K. Minami, "Structural Design for Dynamic Loads," McGraw Hill Book Co., Inc. New York, 1959, p. 135-136.
15. W. J. Schuman, Jr., "The Response of Cylindrical Shells to External Blast Loading," BRL Memorandum Report 1461, Ballistic Research Laboratories, Aberdeen Proving Ground, March, 1963.

16. W. J. Schuman, Jr., "The Response of Cylindrical Shells to External Blast Loading -- Part II," BRL Memorandum Report 1560, Ballistic Research Laboratories, Aberdeen Proving Ground, May, 1964.

17. W. J. Schuman, Jr., "A Failure Criterion for Blast Loaded Cylindrical Shells," BRL Rep. 1292, Ballistic Research Laboratories, Aberdeen Proving Ground, May, 1965.

18. H. E. Lindberg. D. L Anderson, R. D. Firth, L. V. Parker, "Response of Reentry Vehicle - Type Shells to Blast Loads," Stanford Research Institute, Contract AF04(694)-655, September 30, 1965.

19. S. Timoshenko, "Theory of Elasticity," McGraw Hill Book Co., 1934, p. 135.

20. Ref. 19, p. 7.

21. A. Nadai, "Theory of Flow and Fracture of Solids," Vo. 2, McGraw Hill Book Co., New York, 1963, p. 49.

22. A. A. Ilyushin and V. S. Lensky, "Strength of Materials," (Translated into English by J. K. Lusher and S. C. Redshaw, Pergamon Press, New York, 1967, p. 55.

23. A. A. Iliouchine, "Plasticite," (Translated into French by A. Popoff and P. Thome) Editions Eyrolles, Paris, 1956, p. 105, 154.

24. J. F. Bell, "The Physics of Large Deformation of Crystalline Solids," Springer Verlag, New York, 1968, p. 4.

25. Ref. 13, p. 529.

26. Y. C. Fung and E. E. Sechler, "Instability of Thin Elastic Shells," Proc. of the First Symposium on Naval Structural Mechanics, Pergamon Press, New York, 1960, p. 118.

27. Ref. 13, p. 543.

28. J. S. Rinehart and J. Pearson,"Behavior of Metals Under Impulsive Loads," Dover Publications, New York, 1965, p. 23.

29. J.E. Greenspon, "Elastic and Plastic Behavior of Cylindrical Shells Under Dynamic Loads Based on Energy Criteria," J G Eng. Res. Assoc, Con. No. DA 36-034-ORD-3081Rd, Tech. Rep. No. 3, Feb., 1963

30. Errata and Addendum to Ref. 29.

31. J.E.Greenspon,"Collapse, Buckling and Post Failure Behavior of Cylindrical Shells Under Elevated Temperature and Dynamic Loads," J G Eng. Res. Assoc., Contract No. DA-18-001-AMC-707(X), Tech. Rep. No. 6, Nov. 1965.

32. W. Flugge,"Stresses in Shells,"Springer Verlag, Berlin, 1962, p. 107-111.

33. T.E. Reynolds, "Inelastic Lobar Buckling of Cylindrical Shells Under External Hydrostatic Pressure," David Taylor Model Basin Report 1392, Aug., 1960.

34. B. O. Almroth, "Buckling of a Cylindrical Shell Subjected to Nonuniform External Pressure," Journal of Applied Mechanics, December, 1962, Vol. 29, Ser. E, No. 4, p. 675-682.

35. Ref. 9, p. 193.

36. Unpublished Data by W. O. Ewing, Ballistic Research Laboratories, 1965.

## DOCUMENT CONTROL DATA - R&D

*(Security classification of title, body of abstract and indexing annotation must be entered when the overall report is classified)*

| | |
|---|---|
| 1 ORIGINATING ACTIVITY (Corporate author)<br>J G ENGINEERING RESEARCH ASSOCIATES | 2a REPORT SECURITY CLASSIFICATION<br>Unclassified<br>2b GROUP |

3 REPORT TITLE

Theoretical Calculation of Iso-Damage Characteristics

4 DESCRIPTIVE NOTES (Type of report and inclusive dates)

Final Report

5 AUTHOR(S) (Last name, first name, initial)

Greenspon, Joshua E.

| 6 REPORT DATE | 7a. TOTAL NO. OF PAGES | 7b NO OF REFS |
|---|---|---|
| February, 1970 | 41 | 36 |

| | |
|---|---|
| 8a CONTRACT OR GRANT NO.<br>Contract No. DAAD05-69-C-0116 | 9a. ORIGINATOR'S REPORT NUMBER(S)<br>10 |
| b PROJECT NO | |
| c | 9b OTHER REPORT NO(S) (Any other numbers that may be assigned this report) |
| d | |

10 AVAILABILITY/LIMITATION NOTICES THIS DOCUMENT IS SUBJECT TO SPECIAL EXPORT CONTROLS AND EACH TRANSMITTAL TO FOREIGN GOVERNMENTS OR FOREIGN NATIONALS MAY BE MADE ONLY WITH PRIOR APPROVAL OF COMMANDING OFFICER, U. S. ARMY ABERDEEN RESEARCH & DEVELOPMENT CENTER, ABERDEEN PROVING GROUND, MARYLAND 21005.

| | |
|---|---|
| 11 SUPPLEMENTARY NOTES | 12. SPONSORING MILITARY ACTIVITY<br>Ballistic Research Laboratories<br>Aberdeen Proving Ground |

13 ABSTRACT

This report contains methods for constructing iso-damage curves for structures. The results for the cylindrical shell are given in detail. It is shown that by starting with the theory presented here we can derive the empirical relation developed by Johnson several years ago. The theory of damage due to short duration contact explosions is presented and the results are compared with experiment. A series of curves are presented which give the damage sensitivity of cylinders as a function of the ratios of diameter to thickness and length to diameter.

| 14. KEY WORDS | LINK A | | LINK B | | LINK C | |
|---|---|---|---|---|---|---|
| | ROLE | WT | ROLE | WT | ROLE | WT |
| Damage to structures by blast | | | | | | |
| Impulse response of Cylinders | | | | | | |
| Blast Loading and Response | | | | | | |
| Iso-Damage | | | | | | |
| Plastic Deformation of Structures under dynamic loading | | | | | | |

## INSTRUCTIONS

1. ORIGINATING ACTIVITY. Enter the name and address of the contractor, subcontractor, grantee, Department of Defense activity or other organization *(corporate author)* issuing the report.

2*a*. REPORT SECURITY CLASSIFICATION: Enter the overall security classification of the report. Indicate whether "Restricted Data" is included. Marking is to be in accordance with appropriate security regulations.

2*b*. GROUP: Automatic downgrading is specified in DoD Directive 5200.10 and Armed Forces Industrial Manual. Enter the group number. Also, when applicable, show that optional markings have been used for Group 3 and Group 4 as authorized.

3. REPORT TITLE: Enter the complete report title in all capital letters. Titles in all cases should be unclassified. If a meaningful title cannot be selected without classification, show title classification in all capitals in parenthesis immediately following the title.

4. DESCRIPTIVE NOTES: If appropriate, enter the type of report, e.g., interim, progress, summary, annual, or final. Give the inclusive dates when a specific reporting period is covered.

5. AUTHOR(S): Enter the name(s) of author(s) as shown on or in the report. Enter last name, first name, middle initial. If military, show rank and branch of service. The name of the principal author is an absolute minimum requirement.

6. REPORT DATE: Enter the date of the report as day, month, year; or month, year. If more than one date appears on the report, use date of publication.

7*a*. TOTAL NUMBER OF PAGES: The total page count should follow normal pagination procedures, i.e., enter the number of pages containing information.

7*b*. NUMBER OF REFERENCES: Enter the total number of references cited in the report.

8*a*. CONTRACT OR GRANT NUMBER: If appropriate, enter the applicable number of the contract or grant under which the report was written.

8*b*, 8*c*, & 8*d*. PROJECT NUMBER: Enter the appropriate military department identification, such as project number, subproject number, system numbers, task number, etc.

9*a*. ORIGINATOR'S REPORT NUMBER(S). Enter the official report number by which the document will be identified and controlled by the originating activity. This number must be unique to this report.

9*b*. OTHER REPORT NUMBER(S): If the report has been assigned any other report numbers *(either by the originator or by the sponsor)*, also enter this number(s).

10. AVAILABILITY/LIMITATION NOTICES: Enter any limitations on further dissemination of the report, other than those imposed by security classification, using standard statements such as:

(1) "Qualified requesters may obtain copies of this report from DDC."

(2) "Foreign announcement and dissemination of this report by DDC is not authorized."

(3) "U. S. Government agencies may obtain copies of this report directly from DDC. Other qualified DDC users shall request through ______________________."

(4) "U. S. military agencies may obtain copies of this report directly from DDC. Other qualified users shall request through ______________________."

(5) "All distribution of this report is controlled. Qualified DDC users shall request through ______________________."

If the report has been furnished to the Office of Technical Services, Department of Commerce, for sale to the public, indicate this fact and enter the price, if known.

11. SUPPLEMENTARY NOTES: Use for additional explanatory notes.

12. SPONSORING MILITARY ACTIVITY: Enter the name of the departmental project office or laboratory sponsoring *(paying for)* the research and development. Include address.

13. ABSTRACT: Enter an abstract giving a brief and factual summary of the document indicative of the report, even though it may also appear elsewhere in the body of the technical report. If additional space is required, a continuation sheet shall be attached.

It is highly desirable that the abstract of classified report be unclassified. Each paragraph of the abstract shall end with an indication of the military security classification of the information in the paragraph, represented as *(TS)*, *(S)*, *(C)*, or *(U)*.

There is no limitation on the length of the abstract. However, the suggested length is from 150 to 225 words.

14. KEY WORDS: Key words are technically meaningful terms or short phrases that characterize a report and may be used as index entries for cataloging the report. Key words must be selected so that no security classification is required. Identifiers, such as equipment model designation, trade name, military project code name, geographic location, may be used as key words but will be followed by an indication of technical context. The assignment of links, rules, and weights is optional.